

ASSIGNING CONFIDENCE: K-PARTITION ENSEMBLES

Aggelos Semoglou

Department of Informatics, Athens University of Economics and Business, Greece
Archimedes Research Unit, Athena Research Center, Greece
a.semoglou@athenarc.gr

John Pavlopoulos

Department of Informatics, Athens University of Economics and Business, Greece
Archimedes Research Unit, Athena Research Center, Greece
annis@aueb.gr

ABSTRACT

Clustering is widely used for unsupervised structure discovery, yet it offers limited insight into how reliable each individual assignment is. Diagnostics, such as convergence behavior or objective values, may reflect global quality, but they do not indicate whether particular instances are assigned confidently, especially for initialization-sensitive algorithms like k -means. This assignment-level instability can undermine both accuracy and robustness. Ensemble approaches improve global consistency by aggregating multiple runs, but they typically lack tools for quantifying pointwise confidence in a way that combines cross-run agreement with geometric support from the learned cluster structure. We introduce **CAKE** (Confidence in Assignments via K-partition Ensembles), a framework that evaluates each point using two complementary statistics computed over a clustering ensemble: assignment stability and consistency of local geometric fit. These are combined into a single, interpretable score in $[0, 1]$. Our theoretical analysis shows that CAKE remains effective under noise and separates stable from unstable points. Experiments on synthetic and real-world datasets indicate that CAKE effectively highlights ambiguous points and stable core members, providing a confidence ranking that can guide filtering or prioritization to improve clustering quality.

1 INTRODUCTION

Clustering is a fundamental task in unsupervised machine learning, widely used to uncover structure in unlabeled data (Jain et al., 1999; Aggarwal & Reddy, 2013). It has core applications in pattern discovery, exploratory analysis, and decision-making across both scientific and applied domains (Kaufman & Rousseeuw, 2009). However, unlike supervised learning, where confidence estimation techniques such as conformal prediction (Shafer & Vovk, 2007) or calibrated probabilities (Guo et al., 2017) are common, clustering methods typically do not offer reliable confidence scores for individual data point assignments. This makes it difficult to assess assignment trustworthiness, which is particularly important when downstream decisions rely on clustering results.

In practice, clustering algorithms often exhibit sensitivity to initialization, susceptibility to local optima, and vulnerability to noisy or ambiguous data (Xu & Wunsch, 2005). Consequently, outcomes may vary across executions, even under fixed algorithmic settings. For example, k -means (MacQueen, 1967), despite its popularity, can produce divergent results across runs due to random initialization (Bubeck et al., 2009). Practitioners often mitigate this by running the algorithm multiple times with different random seeds and selecting the best result based on internal validation metrics. However, this approach only addresses global variability and offers no insight into the reliability of individual point assignments. Such assignment-level instability is particularly problematic in settings like anomaly detection or scientific discovery, where unreliable assignments can mislead interpretation or obscure important patterns. Moreover, most existing evaluation methods assess clustering quality at a global or cluster level, using objective values or internal validation metrics such as the Silhouette score or Davies–Bouldin index (Arbelaitz et al., 2013; Vendramin et al., 2009).

Ensemble-based techniques like consensus clustering (Strehl & Ghosh, 2002; Zhang, 2022; Aktas Dejaegere et al., 2023) have also been explored to improve robustness by aggregating multiple partitions. However, they still lack interpretable, pointwise confidence scores that capture both cross-run agreement in label assignments and geometric fit. In response, many ensemble-style uncertainty heuristics focus primarily on *agreement*, for example, counting aligned “votes” for each point’s label across runs or measuring dispersion of assignments, to identify unstable samples (Inkaya, 2022; Zhang et al., 2025). While useful, agreement alone does not reveal whether a point is *geometrically* well supported by its assigned cluster, since a point can be consistently assigned due to a systematic bias or an overly rigid decision boundary even when it is isolated or weakly connected to the cluster structure. Conversely, purely geometric signals (such as the Silhouette score) computed within a single run can be overly optimistic in ambiguous regions: a point may appear well placed under that run’s geometry, yet still switch clusters across runs because it lies near a boundary or because multiple partitions explain it nearly equally well (Liu et al., 2022). These complementary failure modes (Fig. 1) motivate a confidence signal that fuses stability and geometry at the point level.

Assignment Stability vs. Geometric Consistency

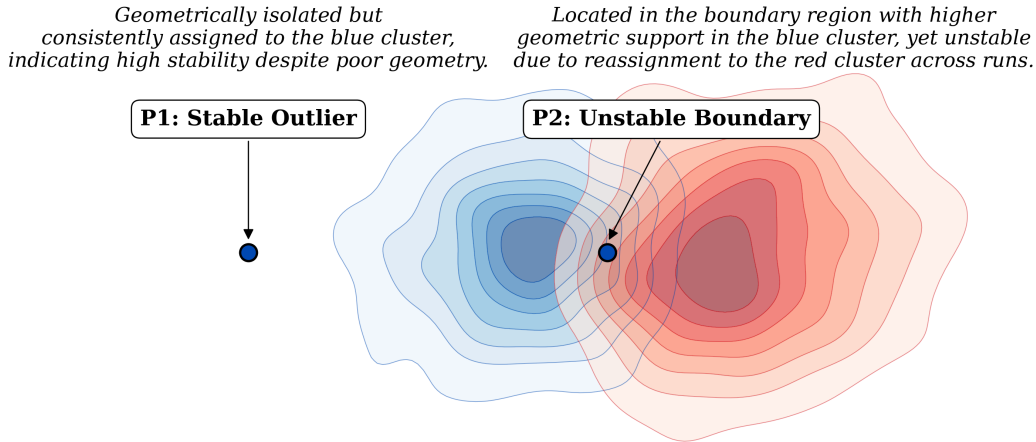


Figure 1: Assignment stability and geometric consistency can fail in complementary ways. P1 (stable outlier; left) is consistently assigned (high stability) despite weak integration into its assigned cluster structure, while P2 (unstable boundary; right) shows higher within-cluster fit to one cluster in a single run yet switches labels across runs near the boundary. These cases suggest that reliable pointwise confidence should account for both signals jointly.

This raises a central question: *How can we assign each data point a confidence score that, across runs, reflects both the assignment stability and the consistency of its geometric support under the learned clustering structure?*

To address this question, we introduce **CAKE** (Confidence in Assignments via K-partition Ensembles), a framework that quantifies per-point confidence by combining two complementary statistics derived from an ensemble of clustering partitions (Fig. 2): (i) pairwise assignment agreement, computed via optimal label alignment using the Hungarian algorithm (Kuhn, 1955; Meila, 2007), and (ii) local geometric consistency, measured through aggregated Silhouette statistics. These components are integrated into a single confidence score in $[0, 1]$ for each point, indicating how strongly its cluster membership is supported and providing a fine-grained ranking that highlights ambiguous points and stable core members. We provide theoretical guarantees for the statistical reliability of CAKE scores and demonstrate, across synthetic and real-world datasets, that CAKE effectively distinguishes between high- and low-confidence assignments. This enables selective filtering or prioritization of points, improving clustering quality and interpretability in a fully label-free setting. CAKE introduces a principled framework for per-instance confidence estimation in clustering, bridging ensemble diversity with pointwise assessment of assignment quality. More broadly, CAKE turns clustering ensembles into a practical, per-point diagnostic that complements global validation.¹

¹Our code on CAKE is publicly available at <https://github.com/semoglou/cake>.

CAKE Framework

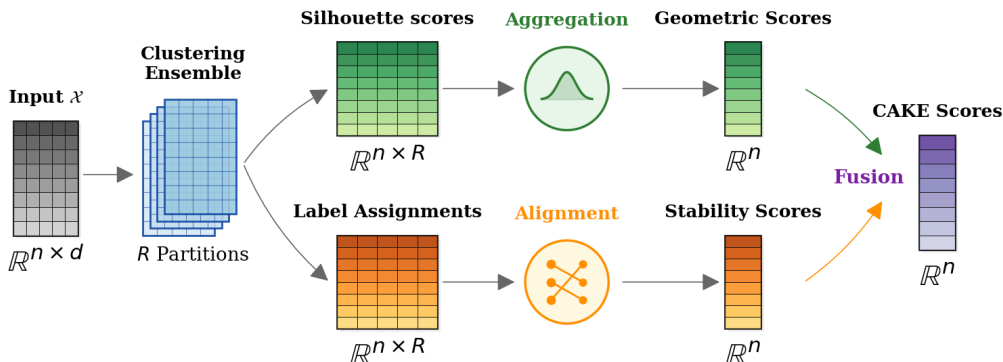


Figure 2: CAKE framework overview. Across an ensemble of R clustering runs (partitions), CAKE aggregates Silhouette statistics into a geometric component and (aligned) label assignments into a stability component, then fuses the two into a confidence score for each data point.

2 RELATED WORK

Assessing the quality of clustering results has been the focus of extensive prior work. Classical validation metrics such as the Silhouette score (Rousseeuw, 1987; Dudek, 2020; Pavlopoulos et al., 2025), Davies–Bouldin index (Davies & Bouldin, 1979), and Calinski–Harabasz criterion (Caliński & Harabasz, 1974) provide global or cluster-level assessments of compactness and separation, but they are not designed to quantify the reliability of individual assignments or to isolate unstable or ambiguous samples within a partition (Arbelaitz et al., 2013).

Clustering ensembles aim to improve robustness by aggregating multiple partitions, using techniques such as co-association matrices or consensus functions (Strehl & Ghosh, 2002; Fred & Jain, 2005; Īnkaya, 2022) and more recent ensemble-selection approaches (Golalipour et al., 2021). While effective at stabilizing global structure, these methods typically do not provide per-point confidence scores (Boongoen & Iam-On, 2018; Zhang, 2022). Their focus lies in producing a single consensus clustering, rather than quantifying how reliably each point is assigned across runs (Topchy et al., 2006). As a result, the consensus output can obscure localized disagreement in regions near cluster boundaries or in heterogeneous areas of the data, making it difficult to identify unstable points. When point-level information is available (e.g., via co-association counts), it is usually an intermediate artifact used to form the consensus rather than an explicit confidence score for diagnosing assignments. Moreover, ensemble aggregation is typically driven by partition agreement and does not incorporate pointwise geometric evidence of assignment quality into the confidence signal.

Efforts to incorporate uncertainty into clustering include fuzzy clustering (Bezdek, 1981; Bezdek et al., 1984), probabilistic mixture models, and bootstrap-based stability analysis (Hennig, 2007; Lange et al., 2004; Ben-Hur et al., 2002; Liu et al., 2022). In related ensemble-stability work, per-point uncertainty is often summarized by the dispersion of aligned label “votes” across runs (e.g., entropy) (Ayad & Kamel, 2008). Recent deep clustering work also studies calibrated cluster confidence, for example via deep clustering networks explicitly trained for confidence calibration (Jia et al., 2025). These approaches provide soft assignments or probability estimates, but may be less interpretable when applied to hard clustering results; in particular, agreement-focused resampling or label-alignment heuristics quantify per-point consistency but omit local geometric fit, leaving no unified stability–geometry measure. In addition, model-based techniques such as Gaussian Mixture Models (Reynolds, 2009) require distributional assumptions, while bootstrapping methods can be computationally intensive and sensitive to sampling variability.

Another relevant area involves the challenge of label alignment when comparing clustering results, often addressed using the Hungarian algorithm for optimal permutation matching (Kuhn, 1955;

Meila, 2007). While this alignment step is standard in ensemble clustering, it has been less commonly used to systematically quantify per-point assignment stability across an ensemble.

Extending these approaches, CAKE combines optimal label alignment with local geometric analysis to provide a principled, interpretable confidence score for each data point, bridging ensemble-based robustness with pointwise reliability and grounding the ensemble consensus in geometric evidence. CAKE draws inspiration from supervised ensemble techniques, where disagreement between classifiers informs uncertainty (Lakshminarayanan et al., 2017; Gal & Ghahramani, 2016; Beluch et al., 2018). Such methods leverage variation across independently trained models or stochastic passes (e.g., dropout) to estimate predictive confidence. In contrast, CAKE operates in an unsupervised regime, using clustering ensemble diversity and within-cluster geometric coherence to infer confidence scores without labels.

3 METHODOLOGY

3.1 SETTING & NOTATION

Assume a dataset $\mathcal{X} = \{x_i\}_{i=1}^n \subset \mathbb{R}^d$ consisting of n data points. Let $\mathcal{C} = \{C^{(1)}, C^{(2)}, \dots, C^{(R)}\}$ denote a collection of R clustering results obtained by repeatedly applying the same clustering algorithm to \mathcal{X} , each time using the same number of clusters k but with a different random seed.

This collection forms a clustering ensemble by capturing multiple partitions of the dataset under stochastic variation. Although all runs use the same algorithm and parameters, random initialization introduces meaningful differences in the resulting partitions, reflecting uncertainty in how individual points are grouped. More generally, the ensemble could be constructed using resampling strategies (e.g., clustering on bootstrapped subsets of \mathcal{X}), or by aggregating partitions from different clustering algorithms, offering a broader perspective on assignment variability (Fig. 4). While our framework is compatible with such (heterogeneous) ensemble construction strategies (Fig. 10), including resampling and multi-algorithm clustering ensembles, in this work, we focus on (homogeneous) ensembles formed by repeated applications of a single clustering method, allowing us to quantify assignment-level confidence without interference from other sources of variation.

To use these partitions quantitatively, we define $\mathcal{L} = \{L^{(1)}, L^{(2)}, \dots, L^{(R)}\}$ as the corresponding set of assignments. Each labeling $L^{(r)} \in \mathcal{L}$ assigns a cluster label to every data point $x_i \in \mathcal{X}$, such that $L^{(r)} = \{L_1^{(r)}, L_2^{(r)}, \dots, L_n^{(r)}\}$, where $L_i^{(r)} \in \{1, 2, \dots, k\}$: the label of x_i in clustering run r .

3.2 ENSEMBLE SILHOUETTE STATISTICS

For each point $x_i \in \mathcal{X}$, let $s_i^{(r)}$ denote its Silhouette score under clustering run $r \in \{1, 2, \dots, R\}$,

$$s_i^{(r)} = \frac{b_i^{(r)} - a_i^{(r)}}{\max\{a_i^{(r)}, b_i^{(r)}\}} \in [-1, 1], \quad (1)$$

which quantifies the quality of its assignment by comparing its average intra-cluster distance $a_i^{(r)}$ to its minimum average inter-cluster distance $b_i^{(r)}$ under clustering run r .

Computing all $s_i^{(r)}$ is $O(n^2d)$ per clustering run. When the base method is centroidal (e.g., k -means, k -means++) and n is large, we compute a centroid-based Silhouette approximation (Wang et al., 2017) by replacing $\tilde{a}_i^{(r)} = \|x_i - \mu_{C_i}^{(r)}\|$ and $\tilde{b}_i^{(r)} = \min_{C \neq C_i} \|x_i - \mu_C^{(r)}\|$, where $\mu_C^{(r)}$ is the centroid of cluster C in run r , and C_i denotes the cluster index of x_i in run r (i.e., $C_i = L_i^{(r)}$). This reduces the per-run cost to $O(nkd)$ while tracking the exact score closely in centroidal settings.

Aggregating over the ensemble. We compute the mean Silhouette score and standard deviation (std) for each point x_i across all R clustering runs in the ensemble:

$$\mu_i = \frac{1}{R} \sum_{r=1}^R s_i^{(r)}, \quad \sigma_i = \sqrt{\frac{1}{R} \sum_{r=1}^R (s_i^{(r)} - \mu_i)^2} \quad (2)$$

We use these two quantities to define a per-point measure of *Silhouette-based reliability*. A high mean μ_i indicates that x_i tends to be well-placed geometrically across clustering runs, while a low std σ_i implies that this quality is consistent. Subtracting σ_i from μ_i penalizes points with high variability in Silhouette values across runs, emphasizing both quality and stability of geometric fit. The resulting score is thresholded at zero to ensure non-negativity²:

$$\tilde{S}_i = (\mu_i - \sigma_i)_+ = \max\{0, (\mu_i - \sigma_i)\} \in [0, 1]. \quad (3)$$

\tilde{S}_i rewards points that not only have high average Silhouette (good cluster fit) but also low variability across runs (stable geometric placement). However, a high \tilde{S}_i does not guarantee that a point is consistently assigned to the same cluster across runs. It only indicates that the point maintains a consistently strong fit within its assigned cluster. To capture actual assignment stability, we introduce a measure based on cluster agreement across the ensemble.

3.3 ENSEMBLE ASSIGNMENT STABILITY

Label alignment. Given two clustering labelings $L^{(r_1)}, L^{(r_2)} \in \mathcal{L}$ from clustering runs r_1, r_2 , the labels may not be aligned: that is, cluster label j in $L^{(r_1)}$ and in $L^{(r_2)}$ may correspond to a different group of points. To align $L^{(r_2)}$ onto $L^{(r_1)}$, we define a contingency matrix $M \in \mathbb{N}^{k \times k}$, where each entry $M_{i,j}$ counts the number of points assigned to cluster i in $L^{(r_1)}$ and cluster j in $L^{(r_2)}$:

$$M_{i,j} = \sum_{p=1}^n \mathbb{1} \left\{ \left(L_p^{(r_1)} = i \right) \wedge \left(L_p^{(r_2)} = j \right) \right\} \quad (4)$$

where $\mathbb{1}(\cdot)$ is the indicator function. Finding the optimal alignment corresponds to finding a permutation $\pi^* : \{1, \dots, k\} \rightarrow \{1, \dots, k\}$ that maximizes agreement:

$$\pi^* = \arg \max_{\pi} \sum_{i=1}^k M_{i,\pi(i)}, \quad (5)$$

where $\pi(i)$ denotes the label in $L^{(r_2)}$ that is matched to label i in $L^{(r_1)}$. This optimization is equivalent to solving a *linear sum assignment problem*, which can be solved using the Hungarian algorithm in $O(k^3)$ time. After aligning $L^{(r_2)}$ onto $L^{(r_1)}$, we denote the aligned labeling by $L^{(r_2 \rightarrow r_1)}$ and define the pointwise agreement between two clustering runs (r_1, r_2) for a data point $x_i \in \mathcal{X}$ as:

$$A_i^{(r_1, r_2)} = \mathbb{1} \left\{ L_i^{(r_1)} = L_i^{(r_2 \rightarrow r_1)} \right\} \in \{0, 1\}. \quad (6)$$

Instance pairwise stability. Given R clustering runs, there are $\binom{R}{2} = \frac{R(R-1)}{2}$ distinct unordered pairs of partitions. We define the pairwise stability score c_i for every point $x_i \in \mathcal{X}$ as the fraction of all unordered run-pairs in which x_i is assigned to the same cluster (after alignment):

$$c_i = \frac{2}{R(R-1)} \sum_{r_1 < r_2} A_i^{(r_1, r_2)} \in [0, 1] \quad (7)$$

By definition, c_i rewards points that are consistently assigned to the same cluster across the ensemble. Points with high c_i exhibit minimal assignment variation and can be viewed as stable members of the underlying clustering structure. Moreover, since $A_i^{(r_1, r_2)}$ is a Bernoulli indicator taking values in $\{0, 1\}$, the quantity c_i is an order-2 U-statistic with a binary (Bernoulli) kernel (Lee, 1990). As such, c_i is an *unbiased estimator of the true pairwise assignment stability* $\mathbb{E}[A_i^{(r_1, r_2)}]$.³

3.4 CAKE SCORE

From the clustering ensemble, we derive two complementary per-instance diagnostics: the assignment-stability estimate c_i (Eq. 7) and the Silhouette-based reliability score \tilde{S}_i (Eq. 3).

²To preserve the signal from consistently negative means (e.g., $\mu_i < 0$ with small σ_i ; a relatively uncommon regime in practice), $\mu_i - \sigma_i$ can be mapped to $[0, 1]$ via $[(\mu_i - \sigma_i) + 1] / 2$.

³Expected agreement over pairs of runs, which reflects how reproducibly x_i is clustered across the ensemble.

The CAKE scores combine these signals into a single confidence value in $[0, 1]$ (outlined in Alg. 1). It rewards observations that are repeatedly assigned to the same cluster across runs and are strongly supported by their local geometry, while penalizing points with unstable assignments or poor local separation from other clusters. Our two formulations are:

$$\text{CAKE}_i^{(\text{PR})} = c_i \tilde{S}_i \quad (8a) \quad \text{CAKE}_i^{(\text{HM})} = \frac{2 c_i \tilde{S}_i}{c_i + \tilde{S}_i} \quad (8b)$$

The product (Eq. 8a) attains high values only when both components are large and rapidly down-weights points that are weak in either stability or geometric fit. The harmonic mean (Eq. 8b) provides a smoother trade-off, remaining sensitive to low values while being less dominated by a single moderate component, which can make the combined score easier to interpret. This mirrors the role of the F1 score in classification, which balances precision and recall via a harmonic mean (Powers, 2011), and similarly treats stability and geometric fit as complementary requirements for high confidence.

Algorithm 1: Compute CAKE Scores

Require: Dataset \mathcal{X} , Clustering algorithm(s) \mathcal{F} , Ensemble size $R > 1$

Ensure: CAKE scores $\forall x_i \in \mathcal{X}$

Initialize label matrix $L \in \mathbb{N}^{n \times R}$

▷ Labels per point/clustering run

Initialize Silhouette score matrix $S \in \mathbb{R}^{n \times R}$

▷ Silhouette per point/clustering run

Initialize Agreement Vector $A \in \mathbb{N}^n$

▷ Pairwise (clustering) run agreements

Clustering Ensemble Construction (§3.1)

for $r = 1$ to R **do**

 Run clustering algorithm \mathcal{F} on \mathcal{X} with random seed r

 Let $L[:, r] \leftarrow$ predicted labels

 Compute Silhouette scores $S[:, r]$ (Eq. 1)

end for

Clustering Ensemble Silhouette Statistics (§3.2)

$\mu \leftarrow \frac{1}{R} \sum_{r=1}^R S[:, r]$, $\sigma \leftarrow \sqrt{\frac{1}{R} \sum_{r=1}^R (S[:, r] - \mu)^2}$ (Eq. 2)

Geometric component $\tilde{S} \leftarrow (\mu - \sigma)_+$ (Eq. 3)

Clustering Ensemble Assignment Stability (§3.3)

for each clustering pair (r_1, r_2) with $r_1 < r_2$ **do**

 Compute optimal label mapping $\pi^{(r_2 \rightarrow r_1)}$ (Eq. 5)

$A \leftarrow A + \mathbb{1} \{L[:, r_1] = \pi^{(r_2 \rightarrow r_1)}(L[:, r_2])\}$ (Eq. 6)

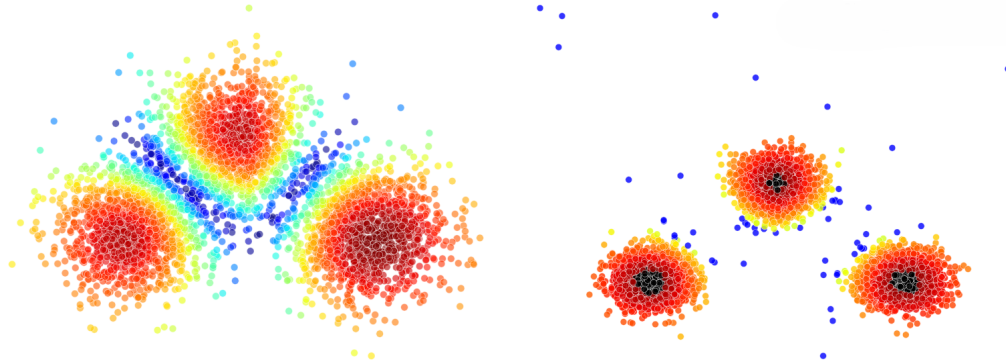
end for

Stability component $c \leftarrow 2A[R(R-1)]^{-1}$ (Eq. 7)

CAKE Scores Computation (§3.4)

$\text{CAKE} \leftarrow \text{CAKE}^{(\text{PR})} = \tilde{S} \odot c$ or $\text{CAKE}^{(\text{HM})} = 2(\tilde{S} \odot c) \oslash (\tilde{S} \oplus c)$ (Eq. 8)

return CAKE



(a) Low \rightarrow high CAKE scores.

(b) Bottom 1% \rightarrow top 90% CAKE scores

Figure 3: CAKE^(PR) (Eq. 8a) scores distribution (left) and percentiles (right) on synthetic data.

Complexity. With the centroid proxy, computing Silhouette scores over R runs costs $O(Rnk d)$, while exact computations cost $O(Rn^2 d)$. Label alignment over all run-pairs builds a $k \times k$ contin-

gency and solves a Hungarian assignment per pair, for $O\left(\binom{R}{2}(n+k^3)\right)$ time; thus CAKE runs in $O(Rnk d + \binom{R}{2}(n+k^3))$ overall, or $O(Rn^2 d + \binom{R}{2}(n+k^3))$ using exact Silhouette scores, and uses $O(nR)$ memory (see runtime vs. R, n on synthetic data in Fig. 12 and Tables 4–5).

Non-convex data. The silhouette component (Eqs. 1–3) is typically computed with euclidean distances and thus favors convex, isotropic clusters. For non-convex structure, euclidean silhouette can be misleading. CAKE accommodates such settings by replacing euclidean distances in the silhouette computation (§3.2) with distances induced by a *positive semidefinite (PSD) kernel*.

Specifically, we use a *kernelized Silhouette* that replaces euclidean distances by RKHS distances to cluster means under a PSD kernel κ :

$$d_{\kappa}^2(x_i, C) = \kappa(x_i, x_i) - \frac{2}{|C|} \sum_{x_j \in C} \kappa(x_i, x_j) + \frac{1}{|C|^2} \sum_{x_p \in C} \sum_{x_q \in C} \kappa(x_p, x_q). \quad (9)$$

Here, $\kappa(\cdot, \cdot)$ is a *positive semidefinite (PSD) kernel*, i.e., a symmetric similarity function such that the Gram matrix $[\kappa(x_i, x_j)]_{i,j}$ is PSD. Intuitively, $\kappa(x, y)$ measures how similar x and y are, and it corresponds to an inner product in some feature space: $\kappa(x, y) = \langle \phi(x), \phi(y) \rangle$.

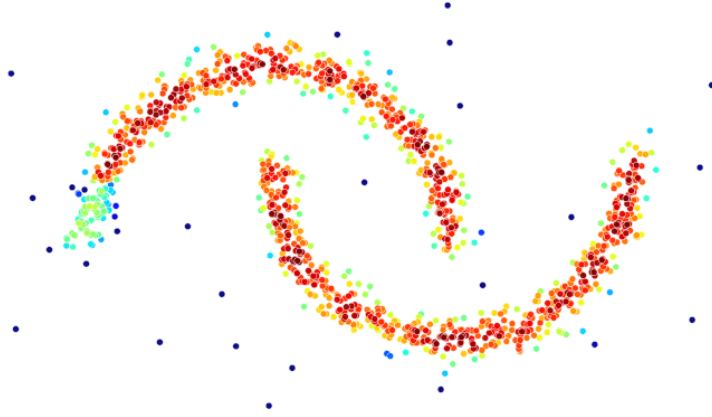


Figure 4: CAKE^(PR) on the two-moons dataset ($n=1200$, noise = 0.06) with 3% uniform outliers. We construct an ensemble of $R=25$ partitions using **spectral clustering** on a k -NN graph, jittering $n_{\text{neighbors}} \in [10, 15]$ per run to induce diversity. For the geometric component we use the kernelized Silhouette (§3.2; Eq. 9) with a self-tuning RBF kernel: $\kappa(x_i, x_j) = \exp(-\|x_i - x_j\|^2 / (\sigma_i \sigma_j))$. We build the Gram matrix K once and reuse it across runs, setting each σ_i to the distance from x_i to its $k_{\text{nn}}=7$ th nearest neighbor. Points are colored by their CAKE scores (\uparrow red, \downarrow blue).

4 THEORETICAL ANALYSIS

We provide two non-asymptotic results for the finite-ensemble stability scores c_i ; full derivations and analogous discussion for the geometric component \tilde{S}_i are given in Appendix A.

4.1 RANKING-ERROR BOUND FOR FINITE ENSEMBLES

Let $R \geq 2$ be the number of independent clustering runs (seeds) performed on \mathcal{X} . For a point $x_i \in \mathcal{X}$ the true pairwise stability is $\theta_i = \mathbb{E} \left[A_i^{(r_1, r_2)} \right]$, where $A_i^{(r_1, r_2)}$ (Eq. 6) is the Bernoulli kernel used in our order-2 U-statistic estimator c_i (Eq. 7). Intuitively, our empirical scores should rank points in the same order as their true stability θ_i and any reversed ordering should be random noise that fades when more runs are added.⁴ The following bound shows how the misordering probability shrinks with R (derivations in Appendix A.1). For any two points $x_i, x_j \in \mathcal{X}$ and margin $\gamma > 0$, it holds:

$$\mathbb{E} \left[A_i^{(r_1, r_2)} \right] \geq \mathbb{E} \left[A_j^{(r_1, r_2)} \right] + \gamma \Rightarrow \Pr [c_i < c_j] \leq 2 \exp \left\{ -R \frac{\gamma^2}{8} \right\}. \quad (10)$$

⁴By standard concentration for bounded U-statistics, c_i converges to θ_i exponentially in R (Appendix A.1).

4.2 FALSE-POSITIVE BOUND FOR UNIFORM-NOISE POINTS

Consider a uniform-noise observation, i.e. a point whose cluster label in each run is drawn independently and uniformly from $\{1, \dots, k\}$. Then $\theta_i = \frac{1}{k}$ and deviations of c_i from θ_i decay exponentially in R (Hoeffding, 1963). Thus, the probability that a noise point falsely attains a high score decreases rapidly with ensemble size (detailed analysis in Appendix A.2):

$$\Pr[c_i > \tau \mid x_i \text{ uniform-noise}] \leq \exp \left\{ -\frac{R}{2} \left(\tau - \frac{1}{k} \right)^2 \right\} \quad \forall \text{ threshold } \tau > \frac{1}{k}. \quad (11)$$

Additionally, if a ϕ fraction of the n observations are uniform-noise, the expected count exceeding $\tau > 1/k$ is at most: $n \cdot \phi \cdot \exp \left\{ -\frac{R}{2} \left(\tau - \frac{1}{k} \right)^2 \right\}$. More generally, for any (possibly non-uniform) label distribution with expected agreement $\theta_i = \mathbb{E}[A_i^{(r_1, r_2)}]$: $\Pr[c_i > \tau] \leq \exp \left\{ -\frac{R}{2} (\tau - \theta_i)^2 \right\}$, (for any threshold $\tau > \theta_i$) so the probability still decays exponentially in R (Appendix A.2).

5 EMPIRICAL VALIDATION

5.1 SYNTHETIC & REAL-WORLD DATASETS

We evaluate CAKE on synthetic and real-world datasets.⁵ The **synthetic datasets** are described next (visualizations in Fig.5). **S1** has 4,000 points sampled from three Gaussian clusters with equal size and std of 2.0; **S2** has 3,000 points from three clusters with std of 2.0, 2.5, and 1.5. **S3** has 4,500 points, where 3,000 belong to three Gaussian clusters with unit std, and 1,500 are uniformly distributed noise points. **S4** has 3,000 points arranged in four wide Gaussian clusters, located at the corners of a square. **S5** has 4,000 points from three clusters with strong density contrast: one tight cluster with std of 0.2, one wide with std of 3.0, and one intermediate with unit std. **S6** has 4,000 points from three clusters with std of 0.4, 2.5, and 0.4, where a sparse central cluster overlaps denser ones on each side. **S7** has 4,000 points, distributed across three clusters of size 500, 1,000, and 2,500, with increasing std of 0.3, 1.5, and 2.5 respectively.

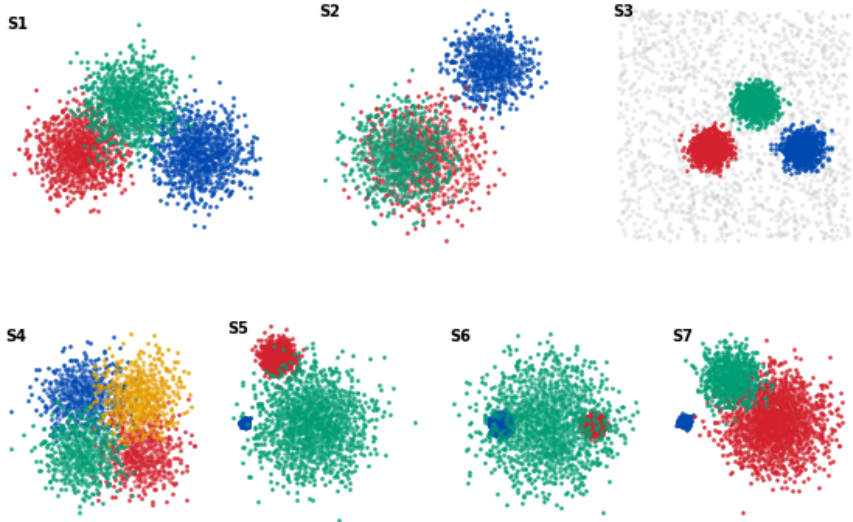


Figure 5: Synthetic datasets (**S1-S7**), colored by ground-truth cluster labels; noise in light gray.

The **real-world datasets** span a wide range of domains and structures (sizes, dimensionality, and preprocessing are summarized in Table 1): **Iris** (IR), **Breast Cancer** (BC), **Pendigits** (PD), **Letter** (LT), **Digits** (DG), **Fashion MNIST** (FM), **Satimage** (SA), and **20 Newsgroups** (NG).

⁵All real-world datasets are publicly available via OpenML (Vanschoren et al., 2013), SCIKIT-LEARN (Pedregosa et al., 2011), or TensorFlow datasets (Abadi et al., 2015).

Dataset (abbrev.)	Modality	n	d	k	Preprocessing / Representation
Iris (IR)	Tabular	150	4	3	None
Breast Cancer (BC)	Tabular	569	10	2	Standardize; PCA
Pendigits (PD)	Tabular	10,992	16	10	None
Letter (LT)	Tabular	20,000	16	26	Standardize
Digits (DG)	Image	1,797	64	10	Flatten 8×8 grayscale images
Fashion MNIST (FM)	Image	60,000	784	10	Flatten 28×28 grayscale images
Satimage (SA)	Remote sensing	6,435	30	6	PCA
20 Newsgroups (NG)	Text	18,846	100	20	all-MiniLM-L6-v2 embeddings; PCA

Table 1: Real datasets. n : number of samples; d : post-preprocessing dim.; k : number of classes.

5.2 EVALUATION SETUP

Instance removal. We remove low-confidence instances based on their CAKE scores (§3.4) and assess the impact on clustering quality. For each dataset, we compute CAKE scores using an ensemble of 20 independent k -means runs at the ground-truth number of clusters k (random initialization for synthetic datasets; k -means++ for real datasets). We use k -means because it is widely used, easy to interpret, and known to be sensitive to initialization, making it a natural candidate for assessing assignment-level confidence; CAKE itself is model-agnostic and applies to any hard-assignment clustering ensemble (see Figs. 4, 10). For each dataset, we form six equal-size subsets, each retaining 70% of the points, $m = \lfloor 0.7n \rfloor$, according to different criteria: **Random** (sample m points uniformly), **Consensus** (top m by across-run label agreement after aligning all runs to a reference-medoid partition, i.e., the most representative run), **\hat{S}** (top m by the Silhouette component; Eq. 3), **\hat{C}** (top m by the stability component; Eq. 7), **CAKE^(PR)** (top m by the product; Eq. 8a), and **CAKE^(HM)** (top m by the harmonic mean; Eq. 8b). While this specific threshold is not necessarily optimal, it offers a reasonable coverage–confidence trade-off (see Fig. 7; Appendix Fig. 13).

We compare clustering performance on the full datasets and on the filtered subsets using new k -means runs (separate from the CAKE ensemble) at the ground-truth k . We measure performance using Adjusted Rand Index (ARI), Adjusted Mutual Information (AMI), and clustering accuracy (ACC), after Hungarian alignment to ground-truth labels. To assess variability, we repeat the evaluation with multiple independent runs and report means with (Student’s t) 95% confidence intervals (Table 2; see Appendix B Tables 10–11 for MiniBatchKMeans and GMM evaluation). Additional results for Silhouette, Normalized Mutual Information (NMI), and the correlation between CAKE score percentiles and clustering accuracy are reported in Appendix B (Table 6).

Convergence. We study how CAKE scores stabilize with ensemble size. For each $R \in \{5, \dots, 70\}$ we draw $B=10$ sub-ensembles of size R , recompute CAKE scores using the centroid-based Silhouette proxy (§3.2), and report the per-point standard deviation across the B estimates (Fig. 6). Lower variability suggests that CAKE scores are stabilizing (converging) as the ensemble grows.

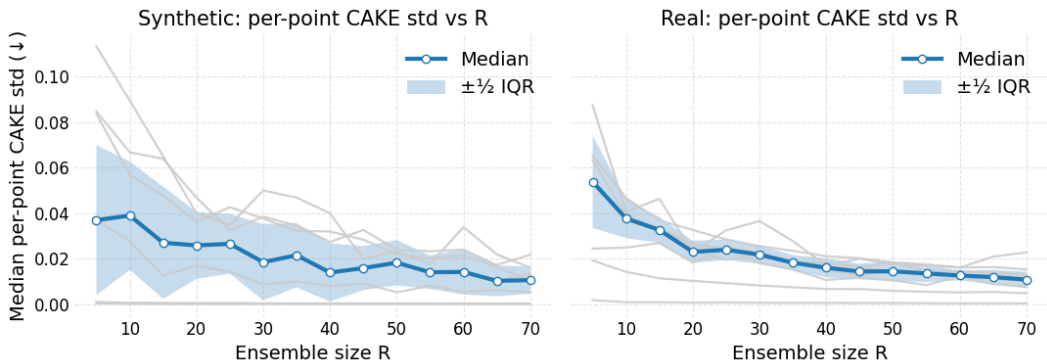


Figure 6: Convergence vs R . Median per-point CAKE^(HM) scores (Eq. 8b) std vs. ensemble size R for synthetic (left) and real (right) datasets. **Lines:** light gray: individual datasets; blue: across-dataset median. **Band:** $\pm \frac{1}{2}$ IQR. Variability drops and stabilizes by $R \approx 30$ –40 across datasets.

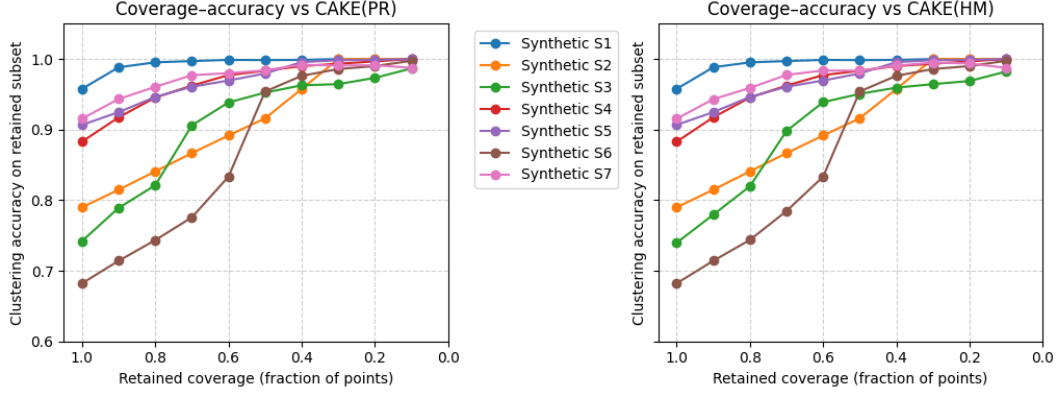
Dataset	Subset	avg ARI	avg AMI	avg ACC
S1	Full	0.879 [0.8785, 0.8791]	0.833 [0.8331, 0.8338]	0.958 [0.9578, 0.9580]
	Random	0.879 [0.8790, 0.8790]	0.834 [0.8339, 0.8339]	0.958 [0.9579, 0.9579]
	Consensus	0.884 [0.8842, 0.8842]	0.839 [0.8394, 0.8394]	0.960 [0.9596, 0.9596]
	C component	0.884 [0.8842, 0.8842]	0.839 [0.8394, 0.8394]	0.960 [0.9596, 0.9596]
	\tilde{S} component	0.992 [0.9921, 0.9921]	0.983 [0.9827, 0.9827]	0.997 [0.9971, 0.9971]
	CAKE ^(PR)	0.992 [0.9921, 0.9921]	0.983 [0.9827, 0.9827]	0.997 [0.9971, 0.9971]
	CAKE ^(HM)	0.992 [0.9921, 0.9921]	0.983 [0.9827, 0.9827]	0.997 [0.9971, 0.9971]
S2	Full	0.552 [0.5225, 0.5812]	0.606 [0.6056, 0.6068]	0.762 [0.6993, 0.8244]
	Random	0.529 [0.4901, 0.5684]	0.601 [0.5923, 0.6102]	0.724 [0.6441, 0.8029]
	Consensus	0.528 [0.5070, 0.5492]	0.628 [0.6031, 0.6530]	0.797 [0.7838, 0.8094]
	C component	0.528 [0.5070, 0.5492]	0.628 [0.6031, 0.6530]	0.797 [0.7838, 0.8094]
	\tilde{S} component	0.679 [0.5731, 0.7840]	0.698 [0.6789, 0.7162]	0.759 [0.6359, 0.8814]
	CAKE ^(PR)	0.680 [0.5741, 0.7860]	0.700 [0.6800, 0.7192]	0.761 [0.6393, 0.8827]
	CAKE ^(HM)	0.680 [0.5738, 0.7858]	0.699 [0.6796, 0.7182]	0.760 [0.6367, 0.8829]
S3	Full	0.498 [0.4941, 0.5016]	0.614 [0.6098, 0.6178]	0.733 [0.7268, 0.7384]
	Random	0.449 [0.3792, 0.5188]	0.580 [0.5352, 0.6255]	0.678 [0.6076, 0.7479]
	Consensus	0.753 [0.7090, 0.7973]	0.757 [0.7301, 0.7836]	0.842 [0.8013, 0.8828]
	C component	0.719 [0.6957, 0.7432]	0.721 [0.7041, 0.7379]	0.830 [0.8128, 0.8473]
	\tilde{S} component	0.795 [0.7667, 0.8241]	0.781 [0.7591, 0.8022]	0.862 [0.8348, 0.8886]
	CAKE ^(PR)	0.734 [0.6444, 0.8232]	0.751 [0.6982, 0.8031]	0.784 [0.7085, 0.8591]
	CAKE ^(HM)	0.784 [0.7538, 0.8137]	0.776 [0.7597, 0.7932]	0.837 [0.8022, 0.8724]
S4	Full	0.716 [0.7158, 0.7167]	0.678 [0.6775, 0.6786]	0.884 [0.8833, 0.8837]
	Random	0.727 [0.7268, 0.7276]	0.693 [0.6926, 0.6933]	0.888 [0.8883, 0.8886]
	Consensus	0.606 [0.5946, 0.6179]	0.598 [0.5939, 0.6029]	0.755 [0.7432, 0.7665]
	C component	0.606 [0.5946, 0.6179]	0.598 [0.5939, 0.6029]	0.755 [0.7432, 0.7665]
	\tilde{S} component	0.902 [0.9022, 0.9022]	0.867 [0.8667, 0.8667]	0.962 [0.9624, 0.9624]
	CAKE ^(PR)	0.902 [0.9022, 0.9022]	0.867 [0.8667, 0.8667]	0.962 [0.9624, 0.9624]
	CAKE ^(HM)	0.902 [0.9022, 0.9022]	0.867 [0.8667, 0.8667]	0.962 [0.9624, 0.9624]
S5	Full	0.593 [0.4434, 0.7435]	0.660 [0.5739, 0.7462]	0.782 [0.6384, 0.9254]
	Random	0.549 [0.3891, 0.7089]	0.634 [0.5415, 0.7267]	0.743 [0.5933, 0.8933]
	Consensus	0.479 [0.4780, 0.4807]	0.570 [0.5689, 0.5710]	0.708 [0.7046, 0.7116]
	C component	0.688 [0.5929, 0.7831]	0.697 [0.6399, 0.7540]	0.867 [0.7988, 0.9355]
	\tilde{S} component	0.840 [0.6821, 0.9980]	0.855 [0.7557, 0.9535]	0.894 [0.7637, 1.0000]
	CAKE ^(PR)	0.908 [0.9075, 0.9075]	0.879 [0.8792, 0.8792]	0.966 [0.9664, 0.9664]
	CAKE ^(HM)	0.925 [0.9245, 0.9245]	0.898 [0.8979, 0.8979]	0.973 [0.9729, 0.9729]
S6	Full	0.303 [0.3006, 0.3045]	0.473 [0.4720, 0.4748]	0.681 [0.6794, 0.6834]
	Random	0.315 [0.2978, 0.3325]	0.480 [0.4690, 0.4920]	0.689 [0.6748, 0.7032]
	Consensus	0.561 [0.5537, 0.5684]	0.586 [0.5780, 0.5943]	0.779 [0.7712, 0.7859]
	C component	0.565 [0.5640, 0.5654]	0.590 [0.5896, 0.5907]	0.782 [0.7815, 0.7828]
	\tilde{S} component	0.566 [0.5506, 0.5811]	0.590 [0.5770, 0.6036]	0.781 [0.7654, 0.7960]
	CAKE ^(PR)	0.558 [0.5302, 0.5860]	0.583 [0.5573, 0.6095]	0.777 [0.7524, 0.8006]
	CAKE ^(HM)	0.573 [0.5662, 0.5798]	0.596 [0.5893, 0.6034]	0.789 [0.7817, 0.7962]
S7	Full	0.615 [0.4786, 0.7523]	0.649 [0.5642, 0.7333]	0.802 [0.6727, 0.9317]
	Random	0.602 [0.4685, 0.7363]	0.636 [0.5464, 0.7253]	0.797 [0.6691, 0.9257]
	Consensus	0.460 [0.4371, 0.4820]	0.545 [0.5385, 0.5519]	0.679 [0.6411, 0.7165]
	C component	0.450 [0.4267, 0.4725]	0.540 [0.5326, 0.5480]	0.668 [0.6329, 0.7035]
	\tilde{S} component	0.713 [0.5401, 0.8869]	0.762 [0.6529, 0.8713]	0.820 [0.6817, 0.9582]
	CAKE ^(PR)	0.861 [0.7566, 0.9662]	0.861 [0.7908, 0.9309]	0.939 [0.8647, 1.0000]
	CAKE ^(HM)	0.678 [0.4982, 0.8581]	0.741 [0.6239, 0.8579]	0.797 [0.6623, 0.9308]
IR	Full	0.692 [0.6255, 0.7580]	0.728 [0.6907, 0.7651]	0.857 [0.7859, 0.9288]
	Random	0.643 [0.5586, 0.7277]	0.697 [0.6525, 0.7425]	0.823 [0.7323, 0.9134]
	Consensus	0.658 [0.5951, 0.7206]	0.733 [0.7047, 0.7620]	0.835 [0.7681, 0.9024]
	C component	0.658 [0.5951, 0.7206]	0.733 [0.7047, 0.7620]	0.835 [0.7681, 0.9024]
	\tilde{S} component	0.824 [0.6491, 0.9985]	0.871 [0.7671, 0.9741]	0.862 [0.7138, 1.0000]
	CAKE ^(PR)	0.855 [0.7552, 0.9541]	0.865 [0.8118, 0.9190]	0.923 [0.8345, 1.0000]
	CAKE ^(HM)	0.874 [0.7222, 1.0000]	0.900 [0.8097, 0.9908]	0.909 [0.7849, 1.0000]

BC	Full	0.663 [0.6558, 0.6698]	0.543 [0.5343, 0.5518]	0.908 [0.9058, 0.9101]
	Random	0.660 [0.6598, 0.6598]	0.534 [0.5337, 0.5337]	0.907 [0.9070, 0.9070]
	Consensus	0.779 [0.7788, 0.7789]	0.679 [0.6773, 0.6815]	0.942 [0.9422, 0.9422]
	C component	0.779 [0.7788, 0.7789]	0.679 [0.6773, 0.6815]	0.942 [0.9422, 0.9422]
	\tilde{S} component	0.754 [0.7543, 0.7543]	0.652 [0.6516, 0.6516]	0.950 [0.9497, 0.9497]
	CAKE ^(PR)	0.754 [0.7543, 0.7543]	0.652 [0.6516, 0.6516]	0.950 [0.9497, 0.9497]
	CAKE ^(HM)	0.754 [0.7543, 0.7543]	0.652 [0.6516, 0.6516]	0.950 [0.9497, 0.9497]
DG	Full	0.630 [0.6032, 0.6568]	0.731 [0.7204, 0.7421]	0.747 [0.7153, 0.7785]
	Random	0.594 [0.5726, 0.6145]	0.712 [0.7009, 0.7240]	0.713 [0.6918, 0.7351]
	Consensus	0.777 [0.7201, 0.8344]	0.835 [0.8094, 0.8614]	0.799 [0.7503, 0.8484]
	C component	0.774 [0.7250, 0.8239]	0.834 [0.8111, 0.8569]	0.784 [0.7296, 0.8376]
	\tilde{S} component	0.763 [0.7175, 0.8092]	0.852 [0.8316, 0.8725]	0.779 [0.7312, 0.8268]
	CAKE ^(PR)	0.741 [0.6807, 0.8013]	0.842 [0.8126, 0.8711]	0.744 [0.6829, 0.8055]
	CAKE ^(HM)	0.793 [0.7466, 0.8392]	0.866 [0.8452, 0.8875]	0.815 [0.7730, 0.8575]
NG	Full	0.352 [0.3421, 0.3610]	0.509 [0.5000, 0.5179]	0.511 [0.4957, 0.5259]
	Random	0.359 [0.3505, 0.3675]	0.516 [0.5080, 0.5232]	0.515 [0.4975, 0.5332]
	Consensus	0.462 [0.4500, 0.4735]	0.586 [0.5819, 0.5895]	0.575 [0.5581, 0.5922]
	C component	0.473 [0.4607, 0.4863]	0.590 [0.5831, 0.5977]	0.578 [0.5586, 0.5973]
	\tilde{S} component	0.467 [0.4437, 0.4903]	0.609 [0.5998, 0.6183]	0.561 [0.5322, 0.5892]
	CAKE ^(PR)	0.494 [0.4766, 0.5123]	0.618 [0.6118, 0.6234]	0.603 [0.5820, 0.6246]
	CAKE ^(HM)	0.467 [0.4437, 0.4903]	0.609 [0.5998, 0.6183]	0.561 [0.5322, 0.5892]
FM	Full	0.353 [0.3416, 0.3641]	0.506 [0.4966, 0.5163]	0.514 [0.4880, 0.5391]
	Random	0.362 [0.3495, 0.3746]	0.509 [0.4994, 0.5193]	0.537 [0.5127, 0.5611]
	Consensus	0.433 [0.4199, 0.4458]	0.560 [0.5533, 0.5666]	0.596 [0.5825, 0.6097]
	C component	0.427 [0.4111, 0.4421]	0.560 [0.5517, 0.5686]	0.596 [0.5742, 0.6177]
	\tilde{S} component	0.447 [0.4295, 0.4637]	0.585 [0.5740, 0.5961]	0.568 [0.5357, 0.5999]
	CAKE ^(PR)	0.445 [0.4149, 0.4744]	0.588 [0.5748, 0.6012]	0.566 [0.5274, 0.6046]
	CAKE ^(HM)	0.474 [0.4467, 0.5007]	0.595 [0.5791, 0.6111]	0.599 [0.5586, 0.6402]
PD	Full	0.541 [0.5121, 0.5690]	0.676 [0.6667, 0.6846]	0.669 [0.6326, 0.7057]
	Random	0.566 [0.5336, 0.5976]	0.682 [0.6725, 0.6917]	0.712 [0.6633, 0.7611]
	Consensus	0.653 [0.6190, 0.6874]	0.734 [0.7210, 0.7467]	0.718 [0.6904, 0.7451]
	C component	0.626 [0.5952, 0.6563]	0.721 [0.7078, 0.7345]	0.704 [0.6768, 0.7316]
	\tilde{S} component	0.754 [0.6854, 0.8226]	0.842 [0.8137, 0.8695]	0.803 [0.7354, 0.8708]
	CAKE ^(PR)	0.724 [0.6749, 0.7740]	0.819 [0.7981, 0.8406]	0.784 [0.7372, 0.8309]
	CAKE ^(HM)	0.759 [0.7166, 0.8010]	0.842 [0.8242, 0.8597]	0.810 [0.7665, 0.8536]
LT	Full	0.152 [0.1456, 0.1577]	0.368 [0.3634, 0.3727]	0.281 [0.2751, 0.2869]
	Random	0.152 [0.1476, 0.1557]	0.373 [0.3675, 0.3794]	0.284 [0.2790, 0.2888]
	Consensus	0.199 [0.1939, 0.2031]	0.430 [0.4264, 0.4333]	0.324 [0.3177, 0.3306]
	C component	0.210 [0.2031, 0.2169]	0.440 [0.4348, 0.4461]	0.333 [0.3230, 0.3434]
	\tilde{S} component	0.213 [0.2034, 0.2234]	0.458 [0.4492, 0.4665]	0.334 [0.3203, 0.3472]
	CAKE ^(PR)	0.219 [0.2096, 0.2277]	0.458 [0.4495, 0.4659]	0.328 [0.3176, 0.3380]
	CAKE ^(HM)	0.222 [0.2163, 0.2267]	0.460 [0.4555, 0.4643]	0.335 [0.3277, 0.3422]
SA	Full	0.510 [0.4657, 0.5550]	0.595 [0.5556, 0.6346]	0.663 [0.6298, 0.6972]
	Random	0.520 [0.4927, 0.5472]	0.608 [0.5895, 0.6273]	0.672 [0.6542, 0.6894]
	Consensus	0.523 [0.4794, 0.5669]	0.575 [0.5549, 0.5945]	0.706 [0.6551, 0.7569]
	C component	0.523 [0.4794, 0.5669]	0.575 [0.5549, 0.5945]	0.706 [0.6551, 0.7569]
	\tilde{S} component	0.710 [0.7080, 0.7125]	0.764 [0.7584, 0.7703]	0.799 [0.7842, 0.8138]
	CAKE ^(PR)	0.682 [0.6383, 0.7249]	0.749 [0.7268, 0.7704]	0.772 [0.7317, 0.8129]
	CAKE ^(HM)	0.653 [0.5997, 0.7067]	0.734 [0.7087, 0.7594]	0.750 [0.6964, 0.8037]

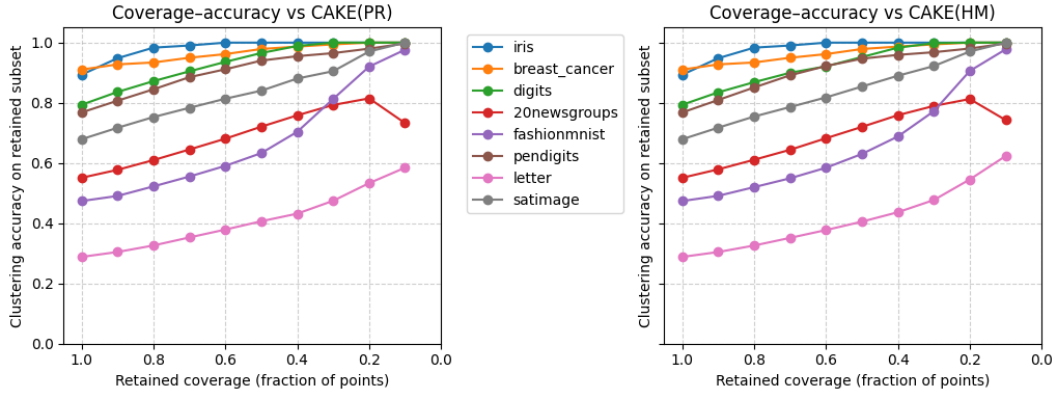
Table 2: ARI, AMI, ACC (clustering accuracy) averages and t -95% confidence intervals, computed over multiple independent clustering runs with varying random seeds. Results are reported for the full datasets (Full) and their filtered subsets mentioned in §5.2. Highest values in **bold**.

Coverage-accuracy evaluation. We evaluate CAKE as a pointwise reliability score for ensemble clustering by measuring clustering accuracy as a function of retained coverage. For each dataset, we compute per-instance CAKE^(PR) and CAKE^(HM) scores from an ensemble of $R=20$ k -means partitions. We then fit a reference k -means solution on the full dataset and evaluate its accuracy against ground truth after optimal label alignment (Hungarian matching). For a grid of coverage

levels $c \in [0.1, 1.0]$, we rank instances by CAKE and measure the reference accuracy restricted to the top- c fraction of instances. Plotting accuracy as a function of coverage yields coverage–accuracy curves, which show how well each CAKE variant orders instances from easier to harder and enables a direct comparison of $\text{CAKE}^{(\text{PR})}$ and $\text{CAKE}^{(\text{HM})}$ (Fig. 7). Sharper curves (higher accuracy at lower coverage) indicate that CAKE concentrates correctly assigned points among the highest scores (see also Appendix B Fig. 13 for a percentile-based clustering accuracy view).



(a) Coverage–accuracy on **synthetic** datasets: S1, S2, S3, S4, S5, S6, S7.



(b) Coverage–accuracy on **real** datasets: IR, BC, DG, NG, FM, PD, LT, SA.

Figure 7: Clustering accuracy on the retained subset as a function of retained coverage, using $\text{CAKE}^{(\text{PR})}$ (left) and $\text{CAKE}^{(\text{HM})}$ (right). Top (7a): synthetic datasets. Bottom (7b): real datasets.

AUROC/AUPRC on consensus correctness. We evaluate CAKE through its ability to distinguish *correctly* clustered instances from *incorrect* ones. For each dataset, we first compute a consensus partition z^* from the clustering ensemble and define a binary correctness label $\mathbb{1}[\pi(z_i^*) = y_i]$, where π denotes the Hungarian alignment mapping from consensus labels to ground-truth classes. Given a confidence score (higher indicates higher reliability), we measure discriminative power using AUROC (area under the ROC curve) and AUPRC (area under the precision-recall curve, i.e., average precision) when predicting $\mathbb{1}[\pi(z_i^*) = y_i] = 1$. We compare four signals: (i) $\text{CAKE}^{(\text{PR})}$ and (ii) $\text{CAKE}^{(\text{HM})}$, which are computed from the same ensemble (Eq. 8a–8b). (iii) *Entropy-based agreement*: for each run r , we align its labels to z^* , yielding aligned labels $\tilde{z}_i^{(r)}$. This induces, for each point, an empirical distribution $p_{i\ell} = \frac{1}{R} \sum_{r=1}^R \mathbb{1}[\tilde{z}_i^{(r)} = \ell]$, with normalized entropy $H_i = -\sum_{\ell=1}^k p_{i\ell} \log(p_{i\ell} + \varepsilon) \Rightarrow \hat{H}_i = 1 - (H_i / \log k)$, so that $\hat{H}_i \in [0, 1]$ is high when aligned votes concentrate on a single label and low when the ensemble is uncertain. (iv) *Bootstrap-based stability*: we draw B subsamples of size $[0.8n]$ and run k -means on each subsample, obtaining partitions $\{z^{(b)}\}_{b=1}^B$. For each point i , we consider all pairs of subsamples (b, b') in which i appears. For each such pair, we align $z^{(b')}$ to $z^{(b)}$ on the points shared by the two subsamples via Hungarian matching, and count whether i receives the same label in the aligned pair. The score is the average

pairwise agreement: $\text{boot}_i = \frac{1}{|\mathcal{P}_i|} \sum_{(b,b') \in \mathcal{P}_i} \mathbb{1}[z_i^{(b)} = \tilde{z}_i^{(b')}]$, where \mathcal{P}_i is the set of subsample-pairs containing i , and $\tilde{z}^{(b')}$ denotes the labels of run b' after alignment to run b . We set $B=20$ to match the default ensemble size $R=20$, yielding a comparable computational budget between baselines. This evaluation (Table 3) quantifies discriminative power at the point level (see Appendix B Tables 7–9 for the same evaluation using MiniBatchKMeans/K-Medoids/GMM instead of k -means). As a complement to Table 3, we test whether each signal yields a monotonic reliability ordering. We bin points by score percentiles and report Spearman’s correlation ($\rho_{\text{Spear.}}$) between percentile rank and within-bin clustering accuracy on representative datasets (S6, S7, BC, DG, PD, LT; Fig. 8).

Dataset	Metric	CAKE ^(PR)	CAKE ^(HM)	Entropy agreement	Bootstrap stability
S1	AUPRC	0.997	0.997	0.958	0.960
	AUROC	0.932	0.932	0.506	0.519
S2	AUPRC	0.930	0.931	0.785	0.807
	AUROC	0.761	0.764	0.488	0.553
S3	AUPRC	0.932	0.932	0.852	0.819
	AUROC	0.842	0.844	0.723	0.665
S4	AUPRC	0.976	0.976	0.887	0.889
	AUROC	0.843	0.843	0.514	0.528
S5	AUPRC	0.978	0.980	0.904	0.908
	AUROC	0.823	0.834	0.499	0.509
S6	AUPRC	0.923	0.924	0.763	0.754
	AUROC	0.821	0.823	0.657	0.621
S7	AUPRC	0.975	0.977	0.933	0.919
	AUROC	0.817	0.826	0.602	0.575
IR	AUPRC	0.977	0.984	0.859	0.923
	AUROC	0.840	0.888	0.328	0.675
BC	AUPRC	0.971	0.971	0.915	0.929
	AUROC	0.773	0.773	0.555	0.636
DG	AUPRC	0.909	0.912	0.734	0.869
	AUROC	0.767	0.777	0.526	0.717
NG	AUPRC	0.638	0.624	0.623	0.637
	AUROC	0.678	0.670	0.636	0.637
FM	AUPRC	0.758	0.755	0.631	0.751
	AUROC	0.707	0.703	0.667	0.742
PD	AUPRC	0.951	0.954	0.900	0.864
	AUROC	0.857	0.866	0.769	0.718
LT	AUPRC	0.465	0.465	0.402	0.409
	AUROC	0.661	0.664	0.617	0.602
SA	AUPRC	0.890	0.894	0.706	0.725
	AUROC	0.784	0.788	0.560	0.592

Table 3: Per-point *consensus correctness* prediction with CAKE^(PR), CAKE^(HM), entropy-based agreement, and bootstrap-based stability. We report AUPRC and AUROC; Best per row in **bold**.

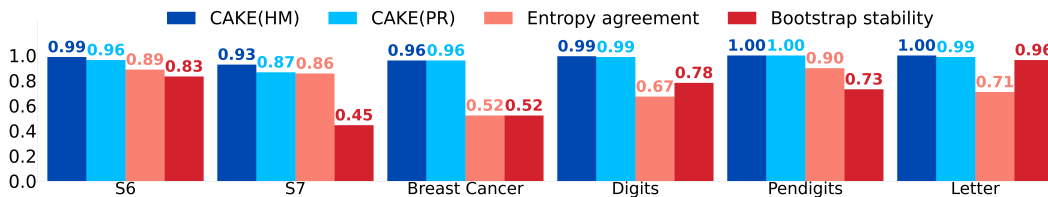


Figure 8: Correlation ($\rho_{\text{Spear.}}$) between confidence-score percentiles and per-bin clustering accuracy.

Error discovery via confidence ranking. We test CAKE for flagging clustering errors. For each dataset we fit a reference k -means++ model at the ground-truth k , align predicted labels to ground truth via Hungarian matching, and mark misclustered points as positives (“errors”). We compare three scores: $\text{CAKE}^{(\text{HM})}$ (Eq. 8b; $R=20$ random k -means runs with centroid-based Silhouette approximation), $\text{GMM } p_{\max}$ (max posterior under a k -component GMM), and their rank-average Fusion. Ranking points from low to high confidence, we report AUPRC on the error class (Fig. 9).

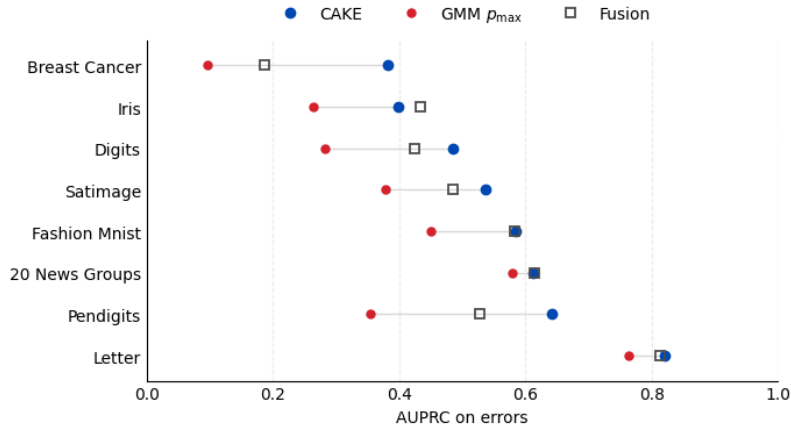


Figure 9: Error discovery via confidence ranking (real datasets) - AUPRC on the error class. Markers show per-dataset AUPRC; light gray connectors join $\text{GMM } p_{\max}$ to CAKE to highlight the per-dataset CAKE score improvement. A simple fusion of these two is marked by \square .

Beyond k -means clustering. CAKE is model-agnostic: it can be applied to ensembles produced by a range of base algorithms. To illustrate this, we compute $\text{CAKE}^{(\text{HM})}$ under three ensemble constructions: (i) homogeneous k -means, (ii) homogeneous GMM, and (iii) heterogeneous k -means+GMM (all with $R=10$), on representative datasets (BC, PD, S5, and S6; Fig. 10).

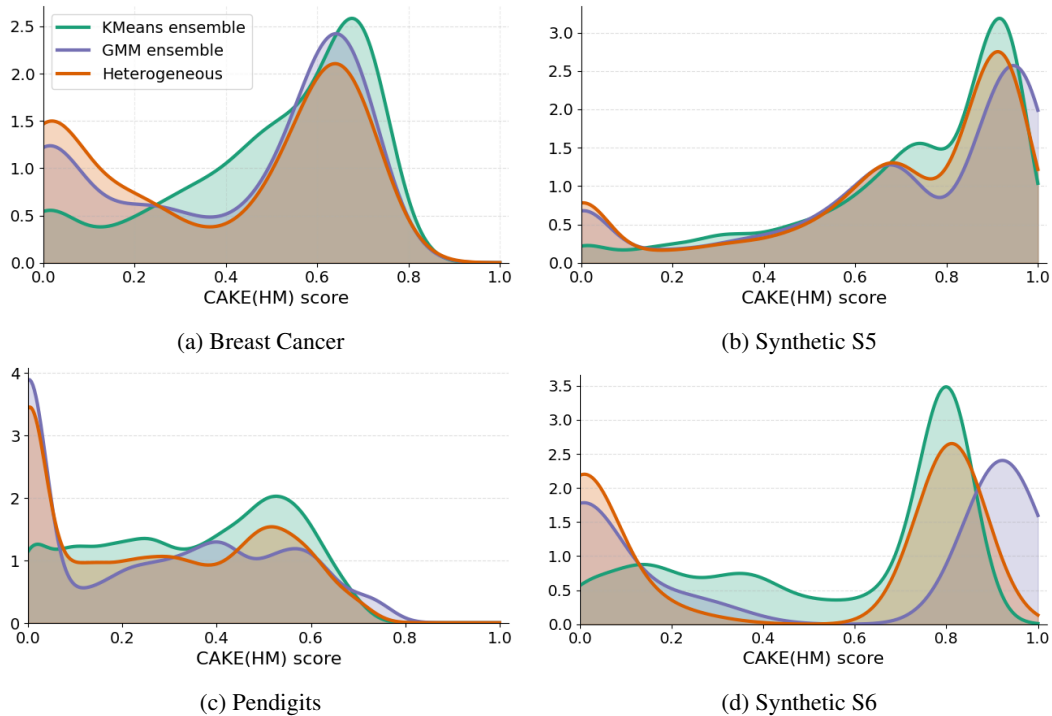


Figure 10: Distributions (KDEs) of $\text{CAKE}^{(\text{HM})}$ (Eq. 8b) under: homogeneous k -means ensembles, homogeneous GMM ensembles, and heterogeneous k -means+GMM ensembles.

Misspecified number of clusters. We test CAKE under cluster-count misspecification, i.e., when the clustering uses a suboptimal number of clusters. For each $k' \in \{k-2, \dots, k+2\}$, where k is the ground-truth number of clusters (Tab. 1), we (i) construct an ensemble of $R=30$ k -means runs with k' clusters and compute $\text{CAKE}^{(\text{HM})}$ scores, and (ii) fit an independent k -means++ model with the same k' for evaluation. We report (a) clustering quality via ARI with respect to ground truth and (b) CAKE ranking quality via AURC (area under the risk–coverage curve), where risk is the misclustering rate after Hungarian alignment. Higher ARI indicates better partitions, while lower AURC indicates that CAKE concentrates correct assignments among high-confidence points (Fig. 11).

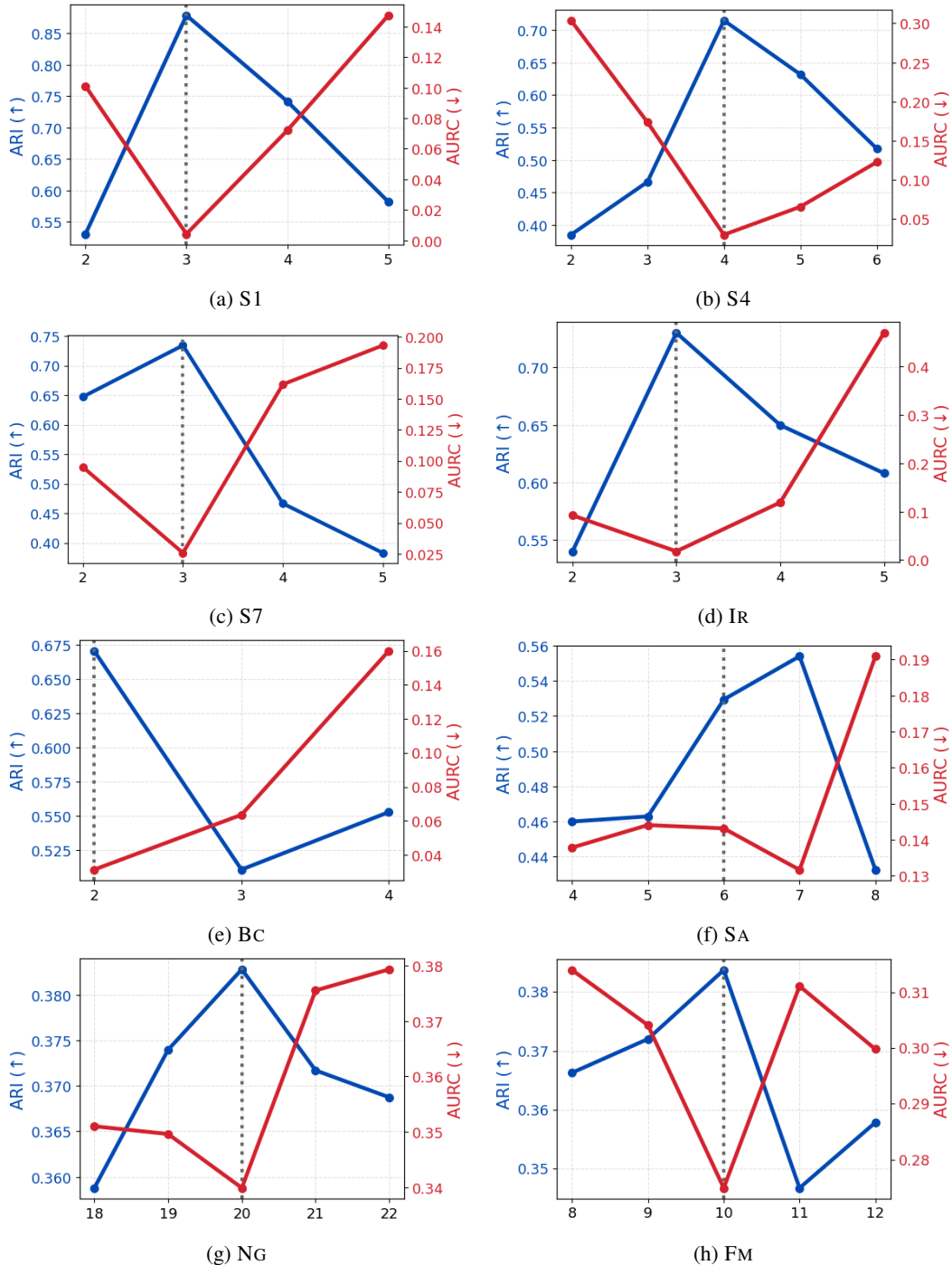


Figure 11: Misspecified k . ARI and AURC vs. k' . Vertical dotted line marks the ground-truth k .

Runtime. We quantify the computational cost of CAKE and the benefit of the centroid-based Silhouette proxy by measuring runtime as a function of ensemble size R and dataset size n on synthetic Gaussian data (Fig. 12). As shown in Fig. 12a (Table 4), runtime grows approximately linearly with R . Figure 12b (Table 5) shows that, when using the centroid-based proxy, runtime scales approximately linearly with n , whereas the exact Silhouette variant increases much more rapidly. Overall, these trends align with our complexity analysis in §3.4 and confirm that the proxy substantially reduces runtime while preserving high agreement with the exact scores (high Pearson correlation and low Mean Absolute Error; Tables 4–5).

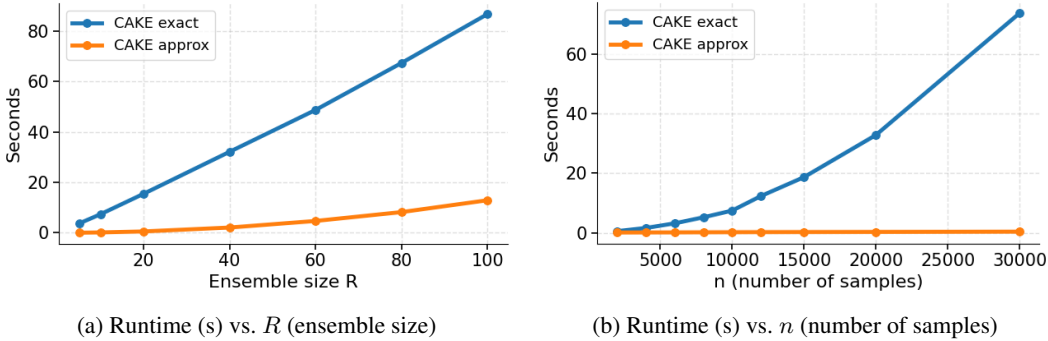


Figure 12: Runtime in seconds (s) for CAKE^(HM) (Eq. 8b) using **exact pairwise Silhouette scores** vs. the **centroid-based Silhouette proxy** on synthetic data. **Left** (a): runtime as a function of ensemble size R ($n=10,000$, $d=20$, $k=10$; exact runtimes are reported in Table 4). **Right** (b): runtime as a function of the number of samples n ($d=20$, $k=10$, $R=20$; exact runtimes are reported in Table 5). Experiments were run on a cloud-hosted notebook with ~ 51 GB RAM.

R	Ensemble construction (s)	CAKE exact (s)	CAKE approx. (s)	Pearson corr.	MAE
5	0.04	3.73	0.05	0.974	0.072
10	0.06	7.42	0.16	0.972	0.069
20	0.13	15.49	0.56	0.975	0.062
40	0.25	32.13	2.10	0.955	0.066
60	0.37	48.71	4.71	0.944	0.061
80	0.49	67.32	8.22	0.936	0.062
100	0.63	86.69	12.91	0.914	0.063

Table 4: Runtime in seconds (s) vs. ensemble size R (Fig. 12a); Pearson correlation and Mean Absolute Error between exact and centroid-based Silhouette-proxy CAKE scores.

n	Ensemble construction (s)	CAKE exact (s)	CAKE approx. (s)	Pearson corr.	MAE
2,000	0.02	0.53	0.06	0.977	0.065
4,000	0.05	1.59	0.08	0.989	0.068
8,000	0.06	5.18	0.14	0.974	0.077
10,000	0.07	7.44	0.17	0.972	0.069
15,000	0.08	18.69	0.22	0.994	0.054
20,000	0.10	32.84	0.26	0.971	0.063
30,000	0.14	73.84	0.35	0.982	0.056

Table 5: Runtime in seconds (s) vs. of number of samples n (Fig. 12b); Pearson correlation and Mean Absolute Error between exact and centroid-based Silhouette-proxy CAKE scores.

5.3 EMPIRICAL RESULTS

Across synthetic and real-world datasets, clustering on the subset retained by CAKE consistently improves ARI, AMI, and ACC relative to using all points (top 70%; Table 2), with similar gains in Silhouette and NMI (Appendix Table 6). These improvements are typically accompanied by tighter confidence intervals, indicating reduced run-to-run variability.

Although the strongest filtering criterion can be dataset-dependent, particularly when geometry (Eq. 3) or stability (Eq. 7) dominates, CAKE (Eq. 8) provides the best overall trade-off: it is best or tied-best for most dataset–metric combinations and remains near the top even when a baseline criterion is optimal on a given dataset (Tables 2, 6).

The component baselines (\tilde{S} , C) can be competitive when one signal is highly informative. For instance, the geometric component alone is strongest on datasets where local separation is the main determinant of cluster assignments (e.g., S3 and SA, where \tilde{S} attains ARI 0.795 and 0.710 respectively), while agreement-focused signals can lead when cross-run consistency is most decisive (e.g., BC, where Consensus/ C perform best in ARI/AMI). However, these signals can fail in complementary ways: a point may be geometrically well-placed in each run but switch clusters across runs, or be consistently assigned yet weakly supported geometrically (Fig. 1). CAKE reduces these failure modes by requiring both stable assignments and consistent geometric support under the learned cluster structure, yielding a more robust confidence signal than either component alone. CAKE outperforms both components on several synthetic datasets (S4–S6) and is also the top-performing filtering choice on most real datasets across ARI/AMI/ACC (e.g., CAKE^(HM) on DG, FM, PD, and LT; CAKE^(PR) on NG). Overall, these trends further support the central claim that combining stability and geometry yields a more reliable confidence ranking than either component alone.

CAKE produces an informative pointwise ranking. Coverage–accuracy curves show that clustering accuracy improves as a function of retained coverage when points are ranked by CAKE scores (Fig. 7), indicating that CAKE concentrates correctly clustered instances among the highest scores. This behavior is also visible in the percentile/decile analysis: accuracy rises nearly monotonically with CAKE score percentiles on both synthetic and real datasets (Appendix Fig. 13). Overall, CAKE behaves as a reliability ordering from ambiguous/borderline points to stable core members.

CAKE enables pointwise correctness prediction and effective error discovery. When predicting whether a consensus assignment is correct (after Hungarian alignment to ground truth), CAKE achieves strong discriminative performance and typically outperforms entropy-based agreement and bootstrap-based stability baselines in both AUPRC and AUROC (Table 3). CAKE also yields a more monotonic reliability ordering: score percentiles correlate strongly with within-bin clustering accuracy (Fig. 8). In error discovery experiments, ranking by CAKE concentrates misclustered points more effectively than GMM posterior confidence p_{\max} on most real datasets, while a simple fusion of the two signals is often competitive (Fig. 9).

CAKE scores stabilize with moderate ensemble sizes. As the ensemble size R increases, per-point score variability steadily decreases and the induced ranking becomes essentially stable, with diminishing returns beyond about $R \approx 30$ –40 (Fig. 6). This indicates that a relatively small ensemble is sufficient to obtain a reliable confidence ordering.

Under misspecified cluster counts, CAKE’s ranking quality also closely tracks clustering quality. Across datasets, ARI typically peaks at (or very near) the ground-truth number of clusters k , and the AURC is minimized at the same (or neighboring) k ; equivalently, the k values that yield the most accurate clustering also yield the sharpest CAKE ranking (Fig. 11).

CAKE is model-agnostic. Across homogeneous k -means, GMM, and heterogeneous k -means & GMM clustering ensembles (as well as spectral clustering ensembles for non-convex geometries; Fig. 4), CAKE score distributions are qualitatively similar and remain informative and well-shaped (Fig. 10), supporting that CAKE behaves consistently beyond purely k -means ensembles. As expected for any ensemble-derived confidence score, CAKE reflects the inductive biases of the base clustering algorithm, since it is intended to measure instance reliability with respect to that procedure and therefore remains comparable across different ensemble constructions.

CAKE is computationally practical. Its runtime follows the expected scaling trends (§3.4). It grows roughly linearly with the ensemble size R and, when using the centroid-based Silhouette proxy, approximately linearly with the dataset size (Fig. 12). The approximation closely matches the exact computation (high correlation and low MAE; Tables 4–5) while substantially reducing cost, making CAKE feasible for large datasets.

6 CONCLUSION

CAKE provides an interpretable, label-free per-point confidence score by fusing cross-run assignment stability with local geometric fit. It is simple to compute from a modest ensemble of standard clustering runs and yields a scalar in $[0, 1]$ for every instance. More broadly, CAKE shows that ensemble diversity, long used for uncertainty estimation in supervised learning, transfers to unsupervised clustering: variability across runs provides a practical per-point confidence signal.

Promising directions include calibrated confidence (e.g., with a small labeled set), integration into semi- and self-supervised pipelines (e.g., uncertainty-aware pseudo-labeling/per-sample weighting), guiding the selection of k via score distributions, and extending CAKE to multi- k clustering ensembles where k varies across runs. By making instance-level uncertainty explicit, CAKE enables more reliable use of clustering in labeling, anomaly detection, and decision pipelines.

REFERENCES

- Martín Abadi, Ashish Agarwal, Paul Barham, Eugene Brevdo, Zhifeng Chen, Craig Citro, Greg S. Corrado, Andy Davis, Jeffrey Dean, Matthieu Devin, Sanjay Ghemawat, Ian Goodfellow, Andrew Harp, Geoffrey Irving, Michael Isard, Yangqing Jia, Rafal Jozefowicz, Lukasz Kaiser, Manjunath Kudlur, Josh Levenberg, Dandelion Mané, Rajat Monga, Sherry Moore, Derek Murray, Chris Olah, Mike Schuster, Jonathon Shlens, Benoit Steiner, Ilya Sutskever, Kunal Talwar, Paul Tucker, Vincent Vanhoucke, Vijay Vasudevan, Fernanda Viégas, Oriol Vinyals, Pete Warden, Martin Wattenberg, Martin Wicke, Yuan Yu, and Xiaoqiang Zheng. TensorFlow: Large-scale machine learning on heterogeneous systems, 2015. URL <https://www.tensorflow.org/>. Software available from [tensorflow.org](https://www.tensorflow.org/).
- Charu C Aggarwal and Chandan K Reddy. *Data Clustering: Algorithms and Applications*. CRC Press, 2013.
- Dilay Aktas Dejaegere, Banu Lokman, Tülin İnkaya, and Gilles Dejaegere. Cluster ensemble selection and consensus clustering: A multi-objective optimization approach. *European Journal of Operational Research*, 314, 10 2023.
- Olatz Arbelaitz, Ibai Gurrutxaga, Javier Muguerza, Jesús M Pérez, and Iñigo Perona. An extensive comparative study of cluster validity indices. *Pattern recognition*, 46(1):243–256, 2013.
- Hanan Ayad and Mohamed S. Kamel. Cumulative voting consensus method for partitions with variable number of clusters. *IEEE transactions on pattern analysis and machine intelligence*, 30: 160–73, 02 2008.
- William H Beluch, Tim Genewein, Andreas Bauer, and Hans Pfister. The power of ensembles for active learning in image classification. In *Proceedings of the IEEE Conference on Computer Vision and Pattern Recognition (CVPR)*, pp. 9368–9377, 2018.
- Asa Ben-Hur, Andre Elisseeff, and Isabelle Guyon. A stability based method for discovering structure in clustered data. *Pacific Symposium on Biocomputing. Pacific Symposium on Biocomputing*, 2002:6–17, 02 2002.
- James Bezdek. *Pattern Recognition With Fuzzy Objective Function Algorithms*. 01 1981. ISBN 978-1-4757-0452-5.
- James C Bezdek, Robert Ehrlich, and William Full. Fcm: The fuzzy c-means clustering algorithm. *Computers & Geosciences*, 10(2-3):191–203, 1984.
- Tossapon Boongoen and Natthakan Iam-On. Cluster ensembles: A survey of approaches with recent extensions and applications. *Computer Science Review*, 28:1–25, 05 2018.
- Sebastien Bubeck, Marina Meila, and Ulrike Luxburg. How the initialization affects the stability of the k-means algorithm. *ESAIM: Probability and Statistics*, 16, 07 2009.
- Tadeusz Caliński and Jerzy Harabasz. A dendrite method for cluster analysis. *Communications in Statistics-theory and Methods*, 3(1):1–27, 1974.

- David L Davies and Donald W Bouldin. A cluster separation measure. *IEEE transactions on pattern analysis and machine intelligence*, (2):224–227, 1979.
- Andrzej Dudek. Silhouette index as clustering evaluation tool. In *Classification and Data Analysis: Theory and Applications 28*, pp. 19–33. Springer, 2020.
- Ana Fred and Anil Jain. Combining multiple clusterings using evidence accumulation. *IEEE transactions on pattern analysis and machine intelligence*, 27:835–50, 07 2005.
- Yarin Gal and Zoubin Ghahramani. Dropout as a bayesian approximation: Representing model uncertainty in deep learning. In *International Conference on Machine Learning*, pp. 1050–1059, 2016.
- Keyvan Gosalipour, Ebrahim Akbari, Seyed Saeed Hamidi, Malrey Lee, and Rasul Enayatifar. From clustering to clustering ensemble selection: A review. *Engineering Applications of Artificial Intelligence*, pp. 104388, 09 2021.
- Chuan Guo, Geoff Pleiss, Yu Sun, and Kilian Q Weinberger. On calibration of modern neural networks. In *International Conference on Machine Learning*, pp. 1321–1330. PMLR, 2017.
- Christian Hennig. Cluster-wise assessment of cluster stability. *Computational Statistics & Data Analysis*, 52:258–271, 09 2007.
- Wassily Hoeffding. Probability inequalities for sums of bounded random variables. *Journal of the American Statistical Association*, 58(301):13–30, 1963.
- Anil K Jain, M Narasimha Murty, and Patrick J Flynn. Data clustering: a review. *ACM Computing Surveys (CSUR)*, 31(3):264–323, 1999.
- Yuheng Jia, Jianhong Cheng, Hui LIU, and Junhui Hou. Towards calibrated deep clustering network. In Y. Yue, A. Garg, N. Peng, F. Sha, and R. Yu (eds.), *International Conference on Representation Learning*, pp. 102968–102992, 2025.
- Leonard Kaufman and Peter J Rousseeuw. *Finding Groups in Data: An Introduction to Cluster Analysis*. Wiley-Interscience, 2009.
- Harold W Kuhn. The hungarian method for the assignment problem. *Naval Research Logistics Quarterly*, 2(1-2):83–97, 1955.
- Balaji Lakshminarayanan, Alexander Pritzel, and Charles Blundell. Simple and scalable predictive uncertainty estimation using deep ensembles. In *Advances in Neural Information Processing Systems*, volume 30, 2017.
- Tilman Lange, Volker Roth, Mikio Braun, and Joachim Buhmann. Stability-based validation of clustering solutions. *Neural Computation*, 16:1299–1323, 06 2004.
- A. J. Lee. *U-Statistics: Theory and Practice*. Marcel Dekker, New York, 1990.
- Tianmou Liu, Han Yu, and Rachael Blair. Stability estimation for unsupervised clustering: A review. *WIREs Computational Statistics*, 14, 01 2022.
- J.B. MacQueen. Some methods for classification and analysis of multivariate observations. In *Proceedings of the 5th Berkeley Symposium on Mathematical Statistics and Probability*, pp. 281–297, 1967.
- Marina Meila. Comparing clusterings – an information based distance. *Journal of Multivariate Analysis*, 98:873–895, 05 2007.
- John Pavlopoulos, Georgios Vardakas, and Aristidis Likas. Revisiting silhouette aggregation. In *Discovery Science*, pp. 354–368, Cham, 2025. Springer Nature Switzerland. ISBN 978-3-031-78977-9.
- Fabian Pedregosa, Gaël Varoquaux, Alexandre Gramfort, Vincent Michel, Bertrand Thirion, Olivier Grisel, Mathieu Blondel, Peter Prettenhofer, Ron Weiss, Vincent Dubourg, et al. Scikit-learn: Machine learning in python. *Journal of Machine Learning Research*, 12, 2011.

- David M. W. Powers. Evaluation: From precision, recall and f-measure to ROC, informedness, markedness & correlation. *Journal of Machine Learning Technologies*, 2:37–63, 2011.
- D.A. Reynolds. Gaussian mixture models. *Encyclopedia of Biometrics*, pp. 659–663, 2009.
- P.J. Rousseeuw. Silhouettes: A graphical aid to the interpretation and validation of cluster analysis. *Journal of Computational and Applied Mathematics*, 20:53–65, 1987.
- Glenn Shafer and Vladimir Vovk. A tutorial on conformal prediction. *Journal of Machine Learning Research*, 9:371–421, 07 2007.
- Alexander Strehl and Joydeep Ghosh. Cluster ensembles - a knowledge reuse framework for combining partitionings. *J Mach Learn Res*, 3, 05 2002.
- Alexander Topchy, Anil Jain, and William Punch. Clustering ensembles: Models of consensus and weak partitions. *IEEE transactions on pattern analysis and machine intelligence*, 27:1866–81, 01 2006.
- Joaquin Vanschoren, Jan N van Rijn, Bernd Bischl, and Luis Torgo. Openml: A collaborative science platform. 2013.
- Lucas Vendramin, Ricardo Campello, and Eduardo Hruschka. On the comparison of relative clustering validity criteria. pp. 733–744, 04 2009.
- Fei Wang, Hector-Hugo Franco-Penya, John D. Kelleher, John Pugh, and Robert Ross. An analysis of the application of simplified silhouette to the evaluation of k-means clustering validity. In Petra Perner (ed.), *Machine Learning and Data Mining in Pattern Recognition*, pp. 291–305, Cham, 2017. Springer International Publishing. ISBN 978-3-319-62416-7.
- Rui Xu and Donald Wunsch. Survey of clustering algorithms. *IEEE Transactions on Neural Networks*, 16(3):645–678, 2005.
- Mimi Zhang. Weighted clustering ensemble: A review. *Pattern Recognition*, 124, 2022. ISSN 0031-3203.
- Xu Zhang, Yuheng Jia, Mofei Song, and Ran Wang. Similarity and Dissimilarity Guided Co-Association Matrix Construction for Ensemble Clustering . *IEEE Transactions on Knowledge & Data Engineering*, 37(11):6694–6707, 2025. ISSN 1558-2191.
- Tülin İnkaya. Consensus similarity graph construction for clustering. *Pattern Analysis and Applications*, 26, 11 2022.

A APPENDIX THEORETICAL ANALYSIS

A.1 MIS-RANKING BOUND

Fix two points $x_i, x_j \in \mathcal{X}$ such that $\theta_i \geq \theta_j + \gamma$ for some margin $\gamma > 0$. Recall that the empirical score c_i (Eq. 7) is an order-2 U-statistic whose (Bernoulli) kernel $A_i^{(r_1, r_2)} \in [0, 1]$ (Eq. 6) has mean $\mathbb{E} \left[A_i^{(r_1, r_2)} \right] = \theta_i$ (§4.1). For each point we define the estimation errors: $e_i = c_i - \theta_i$, $e_j = c_j - \theta_j$. Using Hoeffding's inequality for order-2 U-statistics with a kernel in $[0, 1]$ for e_i, e_j :

$$\Pr(e_i \geq \epsilon) \leq \exp\left(-\frac{R\epsilon^2}{2}\right), \quad \Pr(e_i \leq -\epsilon) \leq \exp\left(-\frac{R\epsilon^2}{2}\right) \quad \forall \epsilon > 0 \text{ (same for } e_j).$$

We choose $\epsilon = \frac{\gamma}{2}$ and define the events: $E_1 = \{e_i \leq -\frac{\gamma}{2}\}$, $E_2 = \{e_j \geq \frac{\gamma}{2}\}$, with probabilities:

$$\Pr(E_1), \Pr(E_2), \text{ which are both bounded above by } \exp\left\{-R\left(\frac{(\gamma/2)^2}{2}\right)\right\} = \exp\left\{-R\frac{\gamma^2}{8}\right\}.$$

If we assume, for contradiction, that the event $\{c_i < c_j\}$ occurs while neither of E_1 nor E_2 takes place.

Then $e_i > -\gamma/2$ and $e_j < \gamma/2$, so that:

$$c_i = \theta_i + e_i \geq \theta_i - \frac{\gamma}{2} \geq \theta_j + \gamma - \frac{\gamma}{2} \geq \theta_j + \frac{\gamma}{2} \geq \theta_j + e_j = c_j \Rightarrow c_i \geq c_j, \text{ which contradicts } c_i < c_j.$$

Therefore, $\{c_i < c_j\} \subseteq E_1 \cup E_2$. Using the bounds on E_1 and E_2 obtained above:

$$\Pr[c_i < c_j] \leq \Pr[E_1] + \Pr[E_2] \leq 2 \exp\left\{-R \cdot \frac{\gamma^2}{8}\right\}.$$

Hence, the probability of a mis-ranking satisfies: $\theta_i - \theta_j \geq \gamma \Rightarrow \Pr[c_i < c_j] \leq 2 \exp\left\{-R\frac{\gamma^2}{8}\right\}$.

A.2 FALSE-STABILITY BOUND

Consider a uniform-noise observation $x_i \in \mathcal{X}$, then for each $L^{(r)} \in \mathcal{L}$, $r \in \{1, \dots, R\}$, its label $L_i^{(r)} \in L^{(r)}$ is drawn independently and uniformly from $\{1, \dots, k\}$. For such a point the Bernoulli kernel in Eq. 6 has expectation:

$$\mathbb{E} \left[A_i^{(r_1, r_2)} \right] = \theta = \frac{1}{k}.$$

Using again Hoeffding's inequality for c_i we get: $\Pr\left[c_i - \mathbb{E} \left[A_i^{(r_1, r_2)} \right] \geq \epsilon\right] \leq \exp\left\{-R\frac{\epsilon^2}{2}\right\}$. We fix a stability threshold $\tau \in \left(\frac{1}{k}, 1\right)$ and select $\epsilon = (\tau - \theta)$. Then, we have:

$$\Pr[c_i > \tau] = \Pr[c_i - \theta > \tau - \theta] \leq \exp\left\{-R\frac{(\tau - \theta)^2}{2}\right\}.$$

Since, x_i is a uniform-noise point: $\theta = 1/k$, and thus:

$$\Pr[c_i > \tau \mid x_i \text{ uniform-noise}] \leq \exp\left\{-\frac{R}{2}\left(\tau - \frac{1}{k}\right)^2\right\}.$$

Additionally, if a fraction $\phi \in (0, 1)$ of the n points of the dataset are uniform-noise, linearity of expectation turns the single-point bound into a dataset bound immediately:

$$\mathbb{E}[\#\{x_i \text{ uniform-noise, } c_i > \tau\}] \leq n \cdot \phi \cdot \exp\left\{-\frac{R}{2}\left(\tau - \frac{1}{k}\right)^2\right\}.$$

In more general scenarios, a noisy observation may be stochastically biased, due to proximity to dominant clusters or algorithmic bias, resulting in a non-uniform label distribution across runs. In such cases, the same concentration bound applies with this generalized $\theta \geq 1/k$:

$$\Pr[c_i > \tau] \leq \exp\left\{-R\frac{(\tau - \theta)^2}{2}\right\}$$

and extends the false-positive bound beyond uniform noise to any setting where labelings follow a known or estimated marginal distribution.

Geometric component. An analogous mis-ranking guarantee holds for the Silhouette-based geometric component. For each point x_i and run $r \in \{1, \dots, R\}$, let $s_i^{(r)} \in [-1, 1]$ denote its (possibly approximated) Silhouette score in run r . The randomness here comes from the clustering procedure (e.g., different random initializations), so for fixed i we view $s_i^{(1)}, \dots, s_i^{(R)}$ as i.i.d. bounded random variables. Let

$$\bar{s}_i := \frac{1}{R} \sum_{r=1}^R s_i^{(r)}, \quad \hat{\sigma}_i^2 := \frac{1}{R} \sum_{r=1}^R (s_i^{(r)} - \bar{s}_i)^2,$$

and recall that the ensemble geometric component used in CAKE is

$$\tilde{S}_i := \max(0, \bar{s}_i - \hat{\sigma}_i)$$

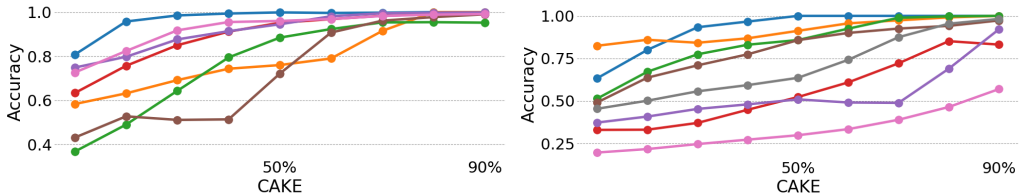
(up to the affine rescaling into $[0, 1]$ described in §3.2). The map

$$(s_i^{(1)}, \dots, s_i^{(R)}) \mapsto \tilde{S}_i$$

is a bounded-differences (Lipschitz) functional of the $s_i^{(r)}$'s, so by standard concentration inequalities for bounded independent variables (e.g., McDiarmid's inequality) \tilde{S}_i concentrates around its population counterpart $g_i := \mathbb{E}[\tilde{S}_i]$ at the usual $1/\sqrt{R}$ rate, with sub-Gaussian tails. Repeating the mis-ranking argument of Appendix A.1, but with c_i and θ_i replaced by \tilde{S}_i and g_i , shows that whenever the true geometric scores of two points differ by a margin $\gamma > 0$ (i.e., $g_i \geq g_j + \gamma$), the probability that CAKE mis-ranks them (i.e., $\tilde{S}_i < \tilde{S}_j$) decays exponentially in $R\gamma^2$. A false-positive bound for \tilde{S}_i can also be derived under additional assumptions on the distribution of Silhouette scores for noise points, again yielding exponentially small probabilities in R .

B APPENDIX RESULTS

Clustering accuracy vs. CAKE percentiles (decile analysis). To complement the coverage–accuracy curves in Fig. 7, we also examine how clustering accuracy varies across CAKE score quantiles. For each dataset, we fit k -means at the ground-truth k , align predicted labels to ground truth via Hungarian matching, partition points into CAKE deciles, and compute accuracy within each decile. This yields an accuracy–percentile trend that summarizes how accuracy changes from the lowest-scored (most ambiguous) instances to the highest-scored (most reliable) instances, providing a decile-level view of CAKE's ranking behavior across the full dataset.



(a) Synthetic datasets: S1, S2, S3, S4, S5, S6, S7. (b) Real datasets: IR, BC, DG, NG, FM, PD, LT, SA.

Figure 13: **Accuracy vs. CAKE score percentile.** Clustering accuracy within CAKE deciles (higher percentiles correspond to higher CAKE scores), after Hungarian alignment to ground-truth labels. This complements Fig. 7 by showing accuracy trends across score quantiles.

Dataset	Subset	avg Silhouette	avg NMI	CORR (CAKE ~ ACC)
S1	Full	0.539 [0.5390, 0.5391]	0.834 [0.8332, 0.8339]	0.881
	Random	0.546 [0.5460, 0.5460]	0.834 [0.8340, 0.8340]	
	Consensus	0.539 [0.5389, 0.5389]	0.839 [0.8395, 0.8395]	
	C component	0.539 [0.5389, 0.5389]	0.839 [0.8395, 0.8395]	
	\tilde{S} component	0.692 [0.6921, 0.6921]	0.983 [0.9828, 0.9828]	
	CAKE ^(PR)	0.692 [0.6921, 0.6921]	0.983 [0.9828, 0.9828]	
	CAKE ^(HM)	0.692 [0.6921, 0.6921]	0.983 [0.9828, 0.9828]	
S2	Full	0.462 [0.4499, 0.4736]	0.606 [0.6059, 0.6070]	0.975
	Random	0.466 [0.4487, 0.4828]	0.602 [0.5927, 0.6105]	
	Consensus	0.459 [0.4499, 0.4673]	0.628 [0.6034, 0.6533]	
	C component	0.459 [0.4499, 0.4673]	0.628 [0.6034, 0.6533]	
	\tilde{S} component	0.582 [0.5254, 0.6394]	0.698 [0.6792, 0.7165]	
	CAKE ^(PR)	0.582 [0.5253, 0.6384]	0.700 [0.6803, 0.7195]	
	CAKE ^(HM)	0.582 [0.5252, 0.6392]	0.699 [0.6799, 0.7185]	
S3	Full	0.537 [0.5270, 0.5472]	0.614 [0.6101, 0.6181]	0.975
	Random	0.503 [0.4694, 0.5357]	0.581 [0.5357, 0.6259]	
	Consensus	0.613 [0.5678, 0.6578]	0.757 [0.7304, 0.7838]	
	C component	0.599 [0.5657, 0.6327]	0.721 [0.7044, 0.7382]	
	\tilde{S} component	0.639 [0.5904, 0.6867]	0.781 [0.7593, 0.8024]	
	CAKE ^(PR)	0.589 [0.5355, 0.6416]	0.751 [0.6986, 0.8033]	
	CAKE ^(HM)	0.613 [0.5858, 0.6407]	0.777 [0.7600, 0.7934]	
S4	Full	0.434 [0.4339, 0.4339]	0.678 [0.6778, 0.6790]	0.999
	Random	0.441 [0.4410, 0.4410]	0.693 [0.6931, 0.6938]	
	Consensus	0.391 [0.3845, 0.3981]	0.599 [0.5946, 0.6036]	
	C component	0.391 [0.3845, 0.3981]	0.599 [0.5946, 0.6036]	
	\tilde{S} component	0.602 [0.6021, 0.6021]	0.867 [0.8669, 0.8669]	
	CAKE ^(PR)	0.602 [0.6021, 0.6021]	0.867 [0.8669, 0.8669]	
	CAKE ^(HM)	0.602 [0.6021, 0.6021]	0.867 [0.8669, 0.8669]	
S5	Full	0.537 [0.4467, 0.6267]	0.660 [0.5741, 0.7463]	0.996
	Random	0.512 [0.4115, 0.6127]	0.634 [0.5419, 0.7268]	
	Consensus	0.495 [0.4943, 0.4951]	0.570 [0.5693, 0.5714]	
	C component	0.582 [0.5298, 0.6349]	0.697 [0.6401, 0.7542]	
	\tilde{S} component	0.724 [0.6001, 0.8486]	0.855 [0.7559, 0.9536]	
	CAKE ^(PR)	0.805 [0.8049, 0.8049]	0.879 [0.8793, 0.8793]	
	CAKE ^(HM)	0.805 [0.8051, 0.8051]	0.898 [0.8980, 0.8980]	
S6	Full	0.511 [0.5106, 0.5116]	0.474 [0.4722, 0.4750]	0.963
	Random	0.512 [0.5075, 0.5157]	0.481 [0.4693, 0.4924]	
	Consensus	0.669 [0.6571, 0.6807]	0.586 [0.5783, 0.5946]	
	C component	0.675 [0.6745, 0.6748]	0.590 [0.5898, 0.5910]	
	\tilde{S} component	0.691 [0.6545, 0.7281]	0.591 [0.5773, 0.6039]	
	CAKE ^(PR)	0.697 [0.6491, 0.7454]	0.584 [0.5576, 0.6098]	
	CAKE ^(HM)	0.717 [0.6936, 0.7396]	0.597 [0.5896, 0.6037]	
S7	Full	0.467 [0.4112, 0.5232]	0.649 [0.5645, 0.7334]	0.984
	Random	0.466 [0.4091, 0.5222]	0.636 [0.5467, 0.7255]	
	Consensus	0.420 [0.4160, 0.4246]	0.546 [0.5389, 0.5523]	
	C component	0.419 [0.4156, 0.4231]	0.541 [0.5330, 0.5484]	
	\tilde{S} component	0.581 [0.5068, 0.6557]	0.762 [0.6531, 0.8714]	
	CAKE ^(PR)	0.643 [0.5941, 0.6913]	0.861 [0.7910, 0.9309]	
	CAKE ^(HM)	0.562 [0.4828, 0.6410]	0.741 [0.6242, 0.8580]	
IR	Full	0.548 [0.5409, 0.5559]	0.731 [0.6947, 0.7679]	0.884
	Random	0.527 [0.5200, 0.5335]	0.703 [0.6592, 0.7470]	
	Consensus	0.537 [0.5191, 0.5550]	0.739 [0.7106, 0.7664]	
	C component	0.537 [0.5191, 0.5550]	0.739 [0.7106, 0.7664]	
	\tilde{S} component	0.637 [0.5766, 0.6971]	0.873 [0.7716, 0.9745]	
	CAKE ^(PR)	0.655 [0.6133, 0.6964]	0.868 [0.8154, 0.9204]	
	CAKE ^(HM)	0.648 [0.5942, 0.7015]	0.902 [0.8134, 0.9909]	

BC	Full	0.357 [0.3560, 0.3574]	0.544 [0.5349, 0.5524]	0.963
	Random	0.360 [0.3599, 0.3599]	0.535 [0.5346, 0.5346]	
	Consensus	0.390 [0.3897, 0.3901]	0.680 [0.6779, 0.6822]	
	C component	0.390 [0.3897, 0.3901]	0.680 [0.6779, 0.6822]	
	\tilde{S} component	0.557 [0.5568, 0.5568]	0.653 [0.6526, 0.6526]	
	CAKE ^(PR)	0.557 [0.5568, 0.5568]	0.653 [0.6526, 0.6526]	
	CAKE ^(HM)	0.557 [0.5568, 0.5568]	0.653 [0.6526, 0.6526]	
DG	Full	0.178 [0.1711, 0.1857]	0.734 [0.7233, 0.7447]	0.996
	Random	0.181 [0.1737, 0.1892]	0.717 [0.7053, 0.7280]	
	Consensus	0.213 [0.1953, 0.2311]	0.838 [0.8123, 0.8635]	
	C component	0.208 [0.1904, 0.2254]	0.837 [0.8140, 0.8591]	
	\tilde{S} component	0.236 [0.2156, 0.2557]	0.854 [0.8341, 0.8744]	
	CAKE ^(PR)	0.230 [0.2110, 0.2482]	0.844 [0.8155, 0.8731]	
	CAKE ^(HM)	0.237 [0.2181, 0.2558]	0.868 [0.8475, 0.8891]	
NG	Full	0.076 [0.0699, 0.0812]	0.511 [0.5016, 0.5194]	0.960
	Random	0.082 [0.0800, 0.0834]	0.518 [0.5103, 0.5254]	
	Consensus	0.105 [0.1021, 0.1072]	0.588 [0.5838, 0.5914]	
	C component	0.106 [0.1028, 0.1094]	0.592 [0.5850, 0.5996]	
	\tilde{S} component	0.108 [0.1047, 0.1118]	0.611 [0.6017, 0.6201]	
	CAKE ^(PR)	0.108 [0.0992, 0.1167]	0.619 [0.6136, 0.6252]	
	CAKE ^(HM)	0.108 [0.1047, 0.1118]	0.611 [0.6017, 0.6201]	
FM	Full	0.142 [0.1373, 0.1476]	0.507 [0.4967, 0.5164]	0.890
	Random	0.140 [0.1341, 0.1458]	0.510 [0.4996, 0.5195]	
	Consensus	0.173 [0.1662, 0.1796]	0.560 [0.5535, 0.5668]	
	C component	0.173 [0.1677, 0.1786]	0.560 [0.5519, 0.5688]	
	\tilde{S} component	0.184 [0.1716, 0.1961]	0.585 [0.5741, 0.5963]	
	CAKE ^(PR)	0.185 [0.1732, 0.1967]	0.588 [0.5750, 0.6014]	
	CAKE ^(HM)	0.192 [0.1812, 0.2023]	0.595 [0.5793, 0.6113]	
PD	Full	0.303 [0.2904, 0.3161]	0.676 [0.6673, 0.6851]	0.999
	Random	0.291 [0.2822, 0.3005]	0.683 [0.6733, 0.6925]	
	Consensus	0.355 [0.3425, 0.3684]	0.734 [0.7217, 0.7473]	
	C component	0.358 [0.3427, 0.3728]	0.722 [0.7085, 0.7351]	
	\tilde{S} component	0.395 [0.3818, 0.4087]	0.842 [0.8141, 0.8698]	
	CAKE ^(PR)	0.379 [0.3548, 0.4028]	0.820 [0.7985, 0.8410]	
	CAKE ^(HM)	0.394 [0.3777, 0.4095]	0.842 [0.8246, 0.8601]	
LT	Full	0.141 [0.1383, 0.1433]	0.371 [0.3665, 0.3757]	0.987
	Random	0.142 [0.1401, 0.1444]	0.378 [0.3719, 0.3838]	
	Consensus	0.185 [0.1816, 0.1880]	0.434 [0.4304, 0.4373]	
	C component	0.190 [0.1864, 0.1938]	0.444 [0.4387, 0.4500]	
	\tilde{S} component	0.193 [0.1892, 0.1976]	0.462 [0.4531, 0.4703]	
	CAKE ^(PR)	0.190 [0.1849, 0.1956]	0.461 [0.4533, 0.4697]	
	CAKE ^(HM)	0.192 [0.1880, 0.1954]	0.464 [0.4593, 0.4681]	
SA	Full	0.349 [0.3378, 0.3605]	0.596 [0.5561, 0.6350]	0.999
	Random	0.348 [0.3350, 0.3602]	0.609 [0.5901, 0.6279]	
	Consensus	0.336 [0.3107, 0.3617]	0.575 [0.5556, 0.5952]	
	C component	0.336 [0.3107, 0.3617]	0.575 [0.5556, 0.5952]	
	\tilde{S} component	0.483 [0.4688, 0.4972]	0.765 [0.7588, 0.7707]	
	CAKE ^(PR)	0.468 [0.4393, 0.4959]	0.749 [0.7272, 0.7708]	
	CAKE ^(HM)	0.443 [0.4104, 0.4765]	0.735 [0.7092, 0.7598]	

Table 6: Average Silhouette and NMI (Normalized Mutual Information) with t -95% confidence intervals and Spearman’s rank correlation of CAKE percentiles with clustering accuracy percentiles. Results are reported for the full datasets (Full) and their filtered subsets mentioned in §5.2. Highest values in **bold**.

Dataset	Metric	CAKE ^(PR)	CAKE ^(HM)	Entropy agreement	Bootstrap stability
S1	AUPRC	0.992	0.993	0.976	0.967
	AUROC	0.884	0.894	0.733	0.619
S2	AUPRC	0.881	0.881	0.801	0.872
	AUROC	0.695	0.692	0.598	0.688
S3	AUPRC	0.943	0.940	0.915	0.868
	AUROC	0.896	0.890	0.879	0.820
S4	AUPRC	0.973	0.974	0.948	0.929
	AUROC	0.835	0.836	0.773	0.697
S5	AUPRC	0.982	0.983	0.917	0.909
	AUROC	0.855	0.856	0.546	0.530
S6	AUPRC	0.919	0.919	0.812	0.766
	AUROC	0.809	0.808	0.720	0.648
S7	AUPRC	0.975	0.977	0.950	0.944
	AUROC	0.836	0.834	0.735	0.650
IR	AUPRC	0.991	0.992	0.962	0.980
	AUROC	0.940	0.941	0.843	0.907
BC	AUPRC	0.961	0.963	0.920	0.936
	AUROC	0.733	0.743	0.584	0.670
DG	AUPRC	0.934	0.931	0.917	0.916
	AUROC	0.815	0.809	0.785	0.771
NG	AUPRC	0.661	0.658	0.682	0.660
	AUROC	0.695	0.693	0.677	0.656
FM	AUPRC	0.743	0.745	0.652	0.713
	AUROC	0.676	0.679	0.643	0.648
PD	AUPRC	0.929	0.929	0.903	0.853
	AUROC	0.844	0.841	0.823	0.769
LT	AUPRC	0.428	0.423	0.415	0.350
	AUROC	0.659	0.656	0.652	0.606
SA	AUPRC	0.876	0.879	0.825	0.870
	AUROC	0.779	0.783	0.716	0.792

Table 7: Per-point consensus correctness prediction (equivalent to Table 3, which uses k -means), using **MiniBatchKMeans**. CAKE scores are computed from an $R=20$ MiniBatchKMeans ensemble; entropy-based agreement ($R=20$) and bootstrap-based stability ($B=20$) are both obtained using MiniBatchKMeans runs. We report AUPRC and AUROC; Highest per row in **bold**.

Dataset	Metric	CAKE ^(PR)	CAKE ^(HM)	Entropy agreement	Bootstrap stability
S1	AUPRC	0.997	0.997	0.964	0.965
	AUROC	0.933	0.933	0.576	0.589
S2	AUPRC	0.928	0.928	0.888	0.794
	AUROC	0.752	0.753	0.720	0.544
S3	AUPRC	0.936	0.935	0.848	0.817
	AUROC	0.853	0.853	0.731	0.673
S4	AUPRC	0.970	0.971	0.906	0.928
	AUROC	0.834	0.837	0.613	0.676
S5	AUPRC	0.979	0.979	0.917	0.908
	AUROC	0.797	0.799	0.504	0.533
S6	AUPRC	0.912	0.912	0.799	0.794
	AUROC	0.686	0.685	0.546	0.532
S7	AUPRC	0.975	0.977	0.939	0.908
	AUROC	0.793	0.805	0.575	0.458
NG	AUPRC	0.316	0.316	0.384	0.335
	AUROC	0.514	0.514	0.591	0.556
BC	AUPRC	0.969	0.967	0.937	0.930
	AUROC	0.726	0.718	0.626	0.601
DG	AUPRC	0.925	0.920	0.934	0.885
	AUROC	0.807	0.798	0.832	0.741
FM	AUPRC	0.770	0.765	0.755	0.693
	AUROC	0.737	0.733	0.764	0.702
IR	AUPRC	0.985	0.986	0.930	0.900
	AUROC	0.895	0.899	0.570	0.466
LT	AUPRC	0.368	0.372	0.373	0.340
	AUROC	0.604	0.605	0.629	0.575
PD	AUPRC	0.942	0.945	0.845	0.897
	AUROC	0.862	0.866	0.725	0.764
SA	AUPRC	0.915	0.913	0.882	0.842
	AUROC	0.815	0.811	0.760	0.680

Table 8: Per-point consensus correctness prediction (equivalent to Table 3, which uses k -means), using **K-Medoids**. CAKE scores are computed from an $R=20$ K-Medoids ensemble; entropy-based agreement ($R=20$) and bootstrap-based stability ($B=20$) are both obtained using K-Medoids runs. We report AUPRC and AUROC; Highest per row in **bold**.

Dataset	Metric	CAKE ^(PR)	CAKE ^(HM)	Entropy agreement	Bootstrap stability
S1	AUPRC	0.997	0.997	0.958	0.960
	AUROC	0.932	0.932	0.503	0.525
S2	AUPRC	0.932	0.932	0.791	0.794
	AUROC	0.766	0.766	0.507	0.515
S3	AUPRC	0.853	0.845	0.945	0.555
	AUROC	0.756	0.747	0.956	0.446
S4	AUPRC	0.976	0.976	0.882	0.895
	AUROC	0.852	0.852	0.510	0.570
S5	AUPRC	0.995	0.995	0.992	0.992
	AUROC	0.568	0.568	0.500	0.531
S6	AUPRC	0.976	0.976	0.967	0.969
	AUROC	0.506	0.506	0.503	0.529
S7	AUPRC	0.982	0.982	0.967	0.953
	AUROC	0.675	0.675	0.542	0.437
IR	AUPRC	0.998	0.998	0.967	0.968
	AUROC	0.949	0.949	0.500	0.537
BC	AUPRC	0.909	0.909	0.692	0.727
	AUROC	0.800	0.800	0.499	0.567
DG	AUPRC	0.947	0.945	0.943	0.926
	AUROC	0.797	0.791	0.799	0.734
NG	AUPRC	0.691	0.684	0.685	0.651
	AUROC	0.711	0.704	0.676	0.634
FM	AUPRC	0.684	0.688	0.572	0.613
	AUROC	0.679	0.683	0.596	0.608
PD	AUPRC	0.898	0.899	0.850	0.891
	AUROC	0.833	0.832	0.833	0.833
LT	AUPRC	0.457	0.452	0.490	0.399
	AUROC	0.628	0.627	0.673	0.586
SA	AUPRC	0.912	0.912	0.596	0.584
	AUROC	0.879	0.879	0.507	0.483

Table 9: Per-point consensus correctness prediction (equivalent to Table 3, which uses k -means), using **GMM**. CAKE scores are computed from an $R=20$ GMM ensemble; entropy-based agreement ($R=20$) and bootstrap-based stability ($B=20$) are both obtained using GMM runs. We report AUPRC and AUROC; Highest per row in **bold**.

Table 10: Average Silhouette, NMI, ARI, AMI, and ACC over multiple independent MiniBatchK-Means runs (different random seeds). Results are reported for the full dataset and for subsets selected by the different filtering strategies (random, consensus-agree, C component, \tilde{S} component, $\text{CAKE}^{(\text{PR})}$, $\text{CAKE}^{(\text{HM})}$). Best performance per dataset and metric is shown in **bold**.

Data	Subset	Clustering results on filtered datasets				
		avg Silhouette	avg NMI	avg ARI	avg AMI	avg ACC
S1	Full	0.486	0.742	0.732	0.742	0.848
	Random	0.546	0.833	0.878	0.833	0.958
	Consensus	0.581	0.858	0.889	0.858	0.937
	C component	0.590	0.864	0.910	0.864	0.959
	\tilde{S} component	0.632	0.928	0.928	0.928	0.952
	$\text{CAKE}^{(\text{PR})}$	0.636	0.950	0.973	0.950	0.990
	$\text{CAKE}^{(\text{HM})}$	0.646	0.955	0.975	0.955	0.991
S2	Full	0.470	0.600	0.499	0.600	0.666
	Random	0.448	0.593	0.537	0.592	0.753
	Consensus	0.553	0.652	0.657	0.652	0.718
	C component	0.509	0.638	0.604	0.638	0.715
	\tilde{S} component	0.562	0.677	0.608	0.676	0.723
	$\text{CAKE}^{(\text{PR})}$	0.580	0.687	0.667	0.686	0.779
	$\text{CAKE}^{(\text{HM})}$	0.578	0.681	0.656	0.681	0.775
S3	Full	0.501	0.588	0.464	0.587	0.700
	Random	0.510	0.604	0.490	0.604	0.719
	Consensus	0.581	0.757	0.763	0.757	0.821
	C component	0.593	0.770	0.782	0.769	0.836
	\tilde{S} component	0.601	0.742	0.716	0.742	0.799
	$\text{CAKE}^{(\text{PR})}$	0.628	0.771	0.774	0.771	0.828
	$\text{CAKE}^{(\text{HM})}$	0.587	0.743	0.729	0.742	0.802
S4	Full	0.420	0.644	0.664	0.644	0.856
	Random	0.435	0.674	0.702	0.674	0.876
	Consensus	0.457	0.728	0.699	0.727	0.789
	C component	0.535	0.796	0.812	0.795	0.900
	\tilde{S} component	0.516	0.785	0.779	0.785	0.859
	$\text{CAKE}^{(\text{PR})}$	0.511	0.777	0.775	0.776	0.854
	$\text{CAKE}^{(\text{HM})}$	0.496	0.765	0.749	0.765	0.840
S5	Full	0.504	0.615	0.532	0.615	0.746
	Random	0.536	0.651	0.579	0.651	0.774
	Consensus	0.614	0.689	0.655	0.689	0.836
	C component	0.620	0.710	0.681	0.710	0.846
	\tilde{S} component	0.745	0.856	0.839	0.855	0.892
	$\text{CAKE}^{(\text{PR})}$	0.815	0.923	0.948	0.923	0.981
	$\text{CAKE}^{(\text{HM})}$	0.779	0.892	0.896	0.892	0.938
S6	Full	0.508	0.481	0.316	0.481	0.687
	Random	0.511	0.486	0.325	0.485	0.690
	Consensus	0.647	0.585	0.566	0.584	0.781
	C component	0.654	0.590	0.570	0.590	0.786
	\tilde{S} component	0.663	0.567	0.541	0.567	0.757
	$\text{CAKE}^{(\text{PR})}$	0.658	0.580	0.555	0.580	0.771
	$\text{CAKE}^{(\text{HM})}$	0.640	0.569	0.546	0.568	0.766
S7	Full	0.419	0.571	0.502	0.571	0.729
	Random	0.384	0.532	0.434	0.532	0.642
	Consensus	0.430	0.587	0.506	0.587	0.703
	C component	0.446	0.613	0.550	0.613	0.720
	\tilde{S} component	0.577	0.787	0.734	0.787	0.810
	$\text{CAKE}^{(\text{PR})}$	0.579	0.801	0.744	0.801	0.820
	$\text{CAKE}^{(\text{HM})}$	0.553	0.773	0.699	0.773	0.778
Full	0.533	0.730	0.682	0.727	0.825	

		Clustering results on filtered datasets				
Data	Subset	avg Silhouette	avg NMI	avg ARI	avg AMI	avg ACC
	Random	0.526	0.715	0.658	0.710	0.844
	Consensus	0.628	0.846	0.829	0.843	0.886
	C component	0.643	0.905	0.894	0.903	0.942
	\tilde{S} component	0.664	0.903	0.879	0.901	0.910
	CAKE ^(PR)	0.664	0.903	0.879	0.901	0.910
	CAKE ^(HM)	0.664	0.903	0.879	0.901	0.910
	Full	0.356	0.537	0.654	0.536	0.905
	Random	0.357	0.532	0.656	0.531	0.906
	Consensus	0.445	0.590	0.707	0.589	0.922
BC	C component	0.445	0.590	0.707	0.589	0.922
	\tilde{S} component	0.496	0.556	0.654	0.555	0.916
	CAKE ^(PR)	0.533	0.608	0.715	0.607	0.937
	CAKE ^(HM)	0.534	0.605	0.707	0.604	0.936
	Full	0.152	0.667	0.536	0.663	0.668
	Random	0.169	0.692	0.566	0.688	0.691
	Consensus	0.199	0.800	0.716	0.797	0.757
DG	C component	0.203	0.819	0.748	0.816	0.781
	\tilde{S} component	0.206	0.816	0.703	0.813	0.731
	CAKE ^(PR)	0.223	0.849	0.767	0.847	0.807
	CAKE ^(HM)	0.219	0.830	0.728	0.828	0.763
	Full	0.068	0.490	0.327	0.488	0.478
	Random	0.069	0.480	0.310	0.477	0.454
	Consensus	0.108	0.613	0.488	0.611	0.575
NG	C component	0.113	0.614	0.480	0.612	0.565
	\tilde{S} component	0.113	0.650	0.518	0.648	0.601
	CAKE ^(PR)	0.113	0.650	0.518	0.648	0.601
	CAKE ^(HM)	0.113	0.650	0.518	0.648	0.601
	Full	0.171	0.505	0.353	0.505	0.515
	Random	0.173	0.499	0.346	0.498	0.510
	Consensus	0.212	0.551	0.414	0.550	0.540
FM	C component	0.226	0.528	0.394	0.527	0.510
	\tilde{S} component	0.226	0.573	0.427	0.573	0.561
	CAKE ^(PR)	0.227	0.578	0.440	0.578	0.557
	CAKE ^(HM)	0.226	0.588	0.456	0.588	0.581
	Full	0.258	0.633	0.488	0.632	0.635
	Random	0.267	0.641	0.501	0.641	0.650
	Consensus	0.360	0.741	0.630	0.740	0.704
PD	C component	0.363	0.762	0.666	0.761	0.733
	\tilde{S} component	0.360	0.782	0.632	0.782	0.703
	CAKE ^(PR)	0.377	0.810	0.718	0.810	0.777
	CAKE ^(HM)	0.356	0.787	0.667	0.787	0.717
	Full	0.128	0.356	0.140	0.353	0.262
	Random	0.122	0.360	0.141	0.356	0.268
	Consensus	0.165	0.425	0.187	0.421	0.311
LT	C component	0.172	0.430	0.191	0.426	0.310
	\tilde{S} component	0.170	0.440	0.202	0.436	0.317
	CAKE ^(PR)	0.169	0.445	0.209	0.442	0.331
	CAKE ^(HM)	0.168	0.439	0.196	0.435	0.313
	Full	0.326	0.571	0.482	0.570	0.641
	Random	0.313	0.561	0.456	0.560	0.640
	Consensus	0.363	0.641	0.559	0.640	0.692
SA	C component	0.366	0.647	0.586	0.647	0.718
	\tilde{S} component	0.437	0.716	0.637	0.715	0.741
	CAKE ^(PR)	0.442	0.720	0.651	0.720	0.742
	CAKE ^(HM)	0.425	0.715	0.650	0.714	0.749

Table 11: Average Silhouette, NMI, ARI, AMI, and ACC over multiple independent GMM runs (different random seeds). Results are reported for the full dataset and for subsets selected by the different filtering strategies (random, consensus-agree, C component, \tilde{S} component, $\text{CAKE}^{(\text{PR})}$, $\text{CAKE}^{(\text{HM})}$). Best performance per dataset and metric is shown in **bold**.

Data	Subset	Clustering results on filtered datasets				
		avg Silhouette	avg NMI	avg ARI	avg AMI	avg ACC
S1	Full	0.539	0.834	0.879	0.834	0.958
	Random	0.546	0.833	0.878	0.833	0.957
	Consensus	0.538	0.836	0.881	0.836	0.959
	C component	0.538	0.836	0.881	0.836	0.959
	\tilde{S} component	0.692	0.983	0.992	0.983	0.997
	$\text{CAKE}^{(\text{PR})}$	0.692	0.983	0.992	0.983	0.997
	$\text{CAKE}^{(\text{HM})}$	0.692	0.983	0.992	0.983	0.997
S2	Full	0.457	0.612	0.566	0.612	0.789
	Random	0.461	0.615	0.562	0.614	0.782
	Consensus	0.489	0.701	0.694	0.700	0.770
	C component	0.489	0.701	0.694	0.700	0.770
	\tilde{S} component	0.613	0.712	0.739	0.712	0.831
	$\text{CAKE}^{(\text{PR})}$	0.615	0.716	0.743	0.716	0.833
	$\text{CAKE}^{(\text{HM})}$	0.615	0.716	0.743	0.716	0.833
S3	Full	0.510	0.617	0.500	0.617	0.720
	Random	0.474	0.616	0.502	0.616	0.717
	Consensus	0.673	0.840	0.864	0.839	0.932
	C component	0.673	0.840	0.864	0.839	0.932
	\tilde{S} component	0.729	0.871	0.906	0.871	0.949
	$\text{CAKE}^{(\text{PR})}$	0.723	0.833	0.857	0.833	0.905
	$\text{CAKE}^{(\text{HM})}$	0.729	0.872	0.907	0.872	0.949
S4	Full	0.434	0.675	0.709	0.675	0.880
	Random	0.441	0.691	0.724	0.691	0.887
	Consensus	0.379	0.619	0.649	0.618	0.806
	C component	0.379	0.619	0.649	0.618	0.806
	\tilde{S} component	0.602	0.866	0.901	0.866	0.962
	$\text{CAKE}^{(\text{PR})}$	0.602	0.866	0.901	0.866	0.962
	$\text{CAKE}^{(\text{HM})}$	0.602	0.866	0.901	0.866	0.962
S5	Full	0.573	0.954	0.973	0.954	0.992
	Random	0.577	0.954	0.972	0.954	0.991
	Consensus	0.457	0.682	0.575	0.681	0.725
	C component	0.457	0.682	0.575	0.681	0.725
	\tilde{S} component	0.827	0.962	0.976	0.962	0.991
	$\text{CAKE}^{(\text{PR})}$	0.827	0.962	0.976	0.962	0.991
	$\text{CAKE}^{(\text{HM})}$	0.827	0.962	0.976	0.962	0.991
S6	Full	0.344	0.852	0.894	0.852	0.966
	Random	0.349	0.855	0.896	0.855	0.967
	Consensus	0.424	0.628	0.546	0.628	0.679
	C component	0.424	0.628	0.546	0.628	0.679
	\tilde{S} component	0.725	0.863	0.895	0.863	0.960
	$\text{CAKE}^{(\text{PR})}$	0.725	0.863	0.895	0.863	0.960
	$\text{CAKE}^{(\text{HM})}$	0.725	0.863	0.895	0.863	0.960
S7	Full	0.476	0.759	0.754	0.759	0.879
	Random	0.510	0.842	0.881	0.842	0.965
	Consensus	0.441	0.601	0.508	0.601	0.710
	C component	0.439	0.601	0.508	0.601	0.703
	\tilde{S} component	0.614	0.832	0.792	0.832	0.862
	$\text{CAKE}^{(\text{PR})}$	0.693	0.921	0.934	0.921	0.980
	$\text{CAKE}^{(\text{HM})}$	0.615	0.826	0.786	0.826	0.858
Full	0.553	0.789	0.750	0.786	0.903	

		Clustering results on filtered datasets				
Data	Subset	avg Silhouette	avg NMI	avg ARI	avg AMI	avg ACC
	Random	0.516	0.756	0.722	0.752	0.894
	Consensus	0.452	0.622	0.544	0.613	0.855
	C component	0.452	0.622	0.544	0.613	0.855
	\tilde{S} component	0.720	0.961	0.979	0.960	0.990
	CAKE ^(PR)	0.720	0.961	0.979	0.960	0.990
	CAKE ^(HM)	0.720	0.961	0.979	0.960	0.990
	Full	0.277	0.031	0.069	0.030	0.649
BC	Random	0.241	0.033	0.074	0.031	0.651
	Consensus	0.291	0.302	0.404	0.301	0.819
	C component	0.291	0.302	0.404	0.301	0.819
	\tilde{S} component	0.292	0.543	0.690	0.542	0.920
	CAKE ^(PR)	0.292	0.543	0.690	0.542	0.920
	CAKE ^(HM)	0.292	0.543	0.690	0.542	0.920
	Full	0.128	0.619	0.498	0.615	0.658
DG	Random	0.132	0.612	0.464	0.604	0.645
	Consensus	0.196	0.808	0.758	0.804	0.779
	C component	0.170	0.794	0.731	0.789	0.735
	\tilde{S} component	0.222	0.834	0.775	0.831	0.770
	CAKE ^(PR)	0.222	0.834	0.775	0.831	0.770
	CAKE ^(HM)	0.222	0.834	0.775	0.831	0.770
	Full	0.071	0.505	0.301	0.503	0.503
NG	Random	0.071	0.505	0.285	0.503	0.489
	Consensus	0.109	0.576	0.430	0.574	0.564
	C component	0.112	0.580	0.438	0.578	0.567
	\tilde{S} component	0.122	0.654	0.514	0.652	0.602
	CAKE ^(PR)	0.122	0.654	0.514	0.652	0.602
	CAKE ^(HM)	0.122	0.654	0.514	0.652	0.602
	Full	0.124	0.521	0.332	0.521	0.510
FM	Random	0.119	0.516	0.325	0.516	0.492
	Consensus	0.222	0.602	0.442	0.602	0.590
	C component	0.230	0.600	0.464	0.600	0.608
	\tilde{S} component	0.258	0.632	0.467	0.631	0.611
	CAKE ^(PR)	0.258	0.632	0.467	0.631	0.611
	CAKE ^(HM)	0.258	0.632	0.467	0.631	0.611
	Full	0.178	0.585	0.425	0.584	0.586
PD	Random	0.184	0.610	0.456	0.609	0.621
	Consensus	0.306	0.745	0.665	0.744	0.713
	C component	0.322	0.753	0.672	0.752	0.715
	\tilde{S} component	0.382	0.814	0.704	0.813	0.772
	CAKE ^(PR)	0.382	0.814	0.704	0.813	0.772
	CAKE ^(HM)	0.382	0.814	0.704	0.813	0.772
	Full	0.036	0.341	0.112	0.338	0.241
LT	Random	0.039	0.356	0.121	0.341	0.252
	Consensus	0.251	0.570	0.357	0.560	0.426
	C component	0.261	0.600	0.382	0.590	0.450
	\tilde{S} component	0.263	0.600	0.384	0.591	0.452
	CAKE ^(PR)	0.281	0.601	0.391	0.592	0.460
	CAKE ^(HM)	0.281	0.601	0.391	0.592	0.460
	Full	0.171	0.575	0.530	0.574	0.660
SA	Random	0.170	0.574	0.496	0.573	0.637
	Consensus	0.169	0.565	0.514	0.565	0.655
	C component	0.169	0.565	0.514	0.565	0.655
	\tilde{S} component	0.409	0.754	0.748	0.754	0.821
	CAKE ^(PR)	0.409	0.754	0.748	0.754	0.821
	CAKE ^(HM)	0.409	0.754	0.748	0.754	0.821